CHAPTER 4 TEM SURVEY

4-1 Outline of Survey

4-1-1 Objective

The objective of TEM survey is to clarify the presence of massive sulfide deposits or vein type deposits and to estimate the sizes and the localities of the deposits.

4-1-2 Exploration method

Transient Electromagnetic (TEM) method

4-1-3 Amounts of TEM survey

Amounts of TEM survey are as follows.

Survey Area	Survey Line	Amount of Measuring Points	
		Fixed Loop	Central Induction
TB-12	7	70	35
TJ-18	5	50	25
TM-27	5	45	20
TO-21	7	77	42
TP-18	7	77	42
Total	31 lines	319 points	164 points

4-2 Survey Method

4-2-1 Methodology

TEM is a transient electromagnetic method, often referred to as time-domain electromagnetic method, in which the ground is energized by a man-made magnetic field and its response is measured as a function of time to determine the resistivity of the earth beneath the observation point as a function of depth. The principle of TEM survey is shown in Figure 2-4-1.

In this method, a steady current is passed through a loop of wire usually situated on or above the surface of the earth that is inductively linked to the earth. The fact that loop sources, which have no direct contact with the earth, can be used makes this method suitable in areas where high surface resistivities prohibit the use of conventional direct current method. This would include regions covered by desert, sand dunes, or extrusive volcanics.

The direct current is abruptly interrupted and the secondary fields due to induced eddy currents can be

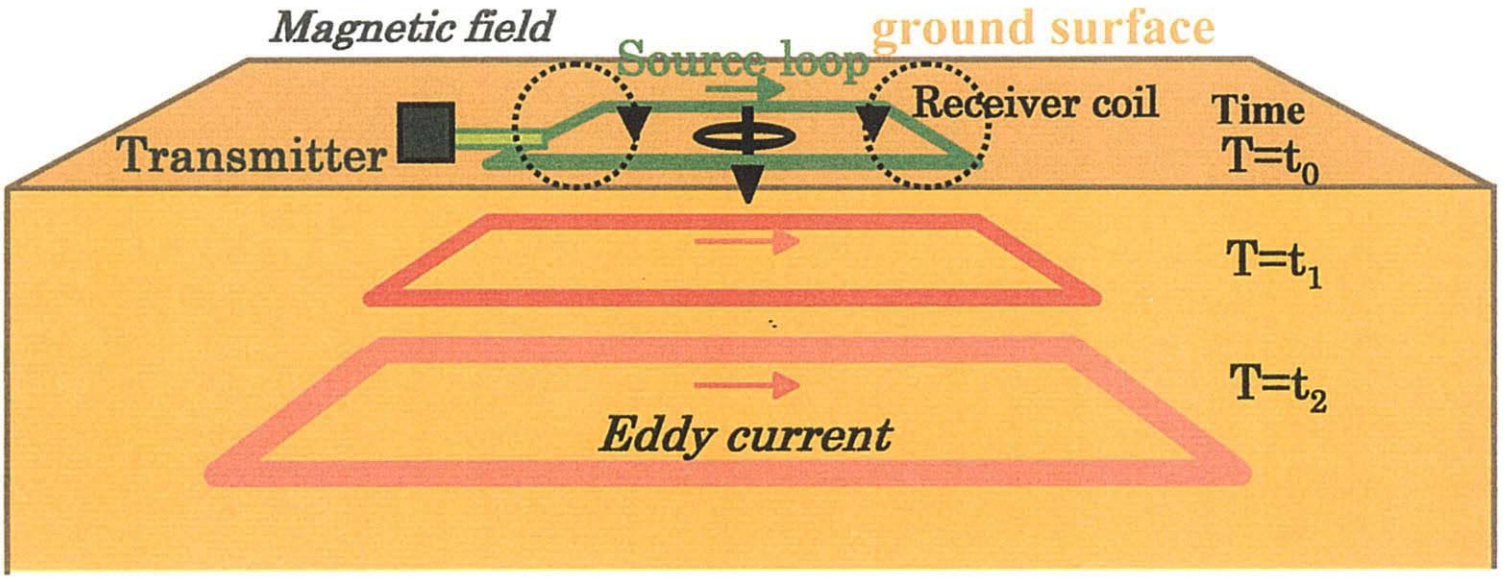

Fig.2-4-1 Principle of TEM Method

measured in the absence of the primary field. The currents migrate from the transmitter into the earth and the pattern resembles a 'smoke ring'. The decay of the magnetic field depends upon the underground resistivity structure. For a poor conductive medium, the receiver coil output voltage, which is proportional to the time rate of change of the secondary magnetic field, is initially large but decays rapidly. The response of a good conductor is initially lower but the voltage decays slower.

The time derivative of the transient magnetic field which results from these currents can be measured by a coil sensor. The decay of the secondary field measured at the surface can be analyzed to determine the resistivity of the earth at depths.

4-2-2 Equipment

The specifications of TEM measurement system manufactured by Geonics Corp., which was used in this survey, are shown in Table 2-4-1.

4-2-3 Field survey

There are several transmitter and receiver configurations of TEM survey. A large fixed transmitter loop configuration was applied for this survey because it is suggested that in the survey area the ore deposit exists in showing vertical vein structure or vertical formational structure. The configuration is shown in Figure 2-4-2.

The specifications of the configuration are as follows.

Transmitter loop size	: 200m × 400m
Interval of measurement line	: 50m (across the estimated deposit)
Interval of measurement point	: 25 m
Transmitter current	: 4.1 amperes
Measurement frequency	: 30 Hz
Sampling time	: 86.7 μ sec to 7.03 msec.
Sampling component	: x, y, z

The central induction measurement was also carried out in order to obtain resistivity values. The interval of measurement points was 50 m.

Table 2-4-1 List of TEM Survey Equipment

ITEM	MODEL	SPECIFICATION
Transmitter	Geonics TEM57 Transmitter	Output Current : 20 A maximum Frequency : 3.0, 7.5, 30 Hz or 2.5, 6.25, 25 Hz Synchronization : Quartz Crystal or Reference Cable Output Voltage : 20 or 44 V Turn-off Time : 115 μ s at 8-turn multi loop Weight : 13 kg
	Geonics TEM47 Transmitter	Output Current : 3.0 A maximum Frequency : 30, 75, 285 Hz or 25, 62.5, 262.5 Hz Synchronization : Reference Cable Output Voltage : 0 to 9 V, continuously current Turn-off Time : 2.5 μ s at 3 A into 40×40m loop Weight : 3.5 kg
Receiver	Geonics PROTEM(D) Receiver	Base Frequency : 0.3, 0.75, 3.0, 7.5, 30, 75, 285 HZ or 0.25, 0.625, 2.5, 6.25, 25, 62.5, 262.5 Hz Time Gate : 20 Dynamic Range : 23 bits (132dB) Memory : 3,300 data-sets Data Transfer : RS232C Power Supply : 12 V rechargeable battery For 8 h continuous operation
EM Sensor	Geonics LF Air-cored Coil Geonics HF Air-cored Coil	Effective Area : 200m^2 Sampling Component : X, Y, Z Frequency : 60 kHz Effective Area : 31.4m^2 Diameter : 1 m Frequency : 1,200 kHz

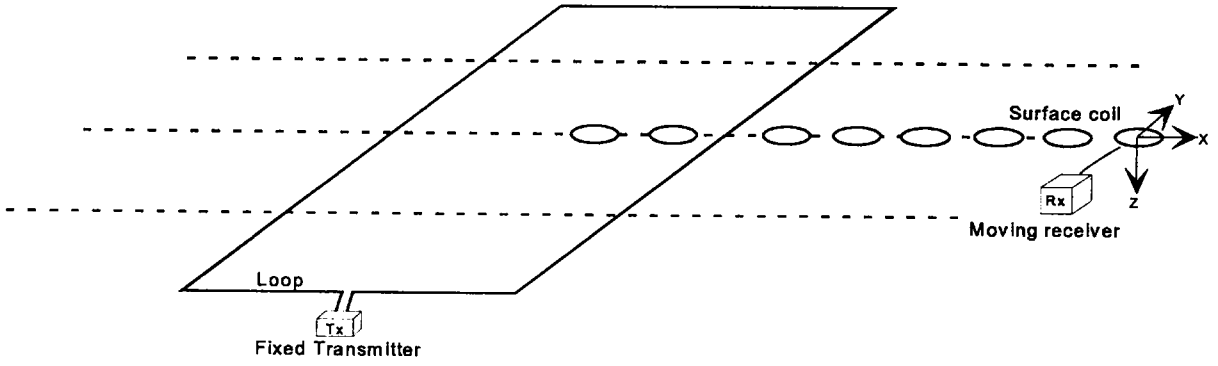

Fig. 2-4-2 Fixed Tx Loop Configuration

There are 20 gates in each time ranges. The channel positions, or gate times, of 20 geometrically spaced time gates are shown in table 2-4-2.

Table 2-4-2 List of Sampling Gate Time

GATE NO.	BASE FREQUENCY 262.5Hz	62.5Hz	25Hz	GATE NO.	BASE FREQUENCY 262.5Hz	62.5Hz	25Hz
1	6.813	35.25	88.13	11	77.94	319.8	799.4
2	8.688	42.75	106.9	12	99.38	405.5	1014
3	11.13	52.50	131.3	13	126.7	514.8	1287
4	14.19	64.75	161.9	14	166.4	654.3	1636
5	18.07	80.25	200.6	15	206.0	832.3	2081
6	23.06	100.3	250.6	16	262.8	1059	2648
7	29.44	125.8	314.4	17	335.2	1349	3373
8	37.56	158.3	395.6	18	427.7	1719	4297
9	47.94	199.8	499.4	19	545.6	2190	5475
10	61.13	252.5	631.3	20	695.9	2792	6978

(unit: μ sec)

4-2-4 Analytical method

The voltages, V_0 (in unit of mV), which are measured by the PROTEM(D) system, are converted to magnetic field decay rate, dB/dt (nV/m^2), using the following formula (Geonics, 1992).

$$\frac{dB}{dt} = \frac{V_0 \cdot 19200}{E \cdot 2^n} \qquad (4\text{-}1)$$

Where E is the receiver coil moment (m^2), and n is the amplitude gain setting. The apparent resistivities $\rho_a(t)$ (ohm-m) as a function of time are then given by,

$$\rho_a(t) \cong \frac{\mu}{4pt_c}\left(\frac{2\mu M}{5t_c\, dB/dt}\right)^{2/3} \qquad (4\text{-}2)$$

Where μ is the magnetic permeability ($4\pi \times 10^{-7}$ H/m), t_c is the measurement time or the gate center time in second, and M is the transmitter moment, which is the product of loop area (m^2) and current (A).

The apparent resistivity is applied to data analysis, one-dimensional inversion, and two-dimensional plate modeling. Two interpretation softwares were "MOTEM" and "TEMIX-XL", were used for two-dimensional plate modeling and one-dimensional inversion respectively.

Many plate parameters are required in the plate modeling analysis which are shown in Figure 2-4-3. In order to estimate the best fitting model, two steps were utilized in this analysis; the first step is fixing the initial model and the second step is changing the location and the conductance of the plate. Conductance is the product of inverse resistivity and thickness, the unit is siemens. For the initial model, the depth of the thin sheet, conductance of the thin sheet and resistivity of the host rock were fixed by the one-dimensional resistivity model. In the initial plate model, the conductance of the plate and length of the plate were determined by geological information of the drill hole (MJSU-2). The strike of the plate, the length and the location of the plate were obtained from the observed voltage distribution map. The dip of the plate was fixed at 90° .

4-3 Survey Results

4-3-1 Test measurement

Test measurement around MJSU-2 (around M-8) was carried out to determine the best transmitter-receiver configuration, measurement line, measurement point and transmitter loop size before starting TEM measurement. The specifications of test measurement are the follows.

(1) Transmitter-receiver configuration

It is known that the ore body exists showing to the vertical vein structure or vertical formational structure by drilling surveys, and that the resistivity of the ore is about 20-30 ohm-m and the resistivity of the host rocks is several thousand ohm-m by laboratory tests. Therefore, the large fixed transmitter loop measurement configuration was applied because of its best coupling with vertical structure target (Fig. 2-4-2).

(2) Measurement profile and point

Measurement profile was set crossing the estimated strike of the vertical ore body. The measurement interval is 25 m and is closer near the anomalous zone.

(3) Transmitter loop size

Loop size was set 200×400 m, considering the length of the estimated ore body and signal intensity.

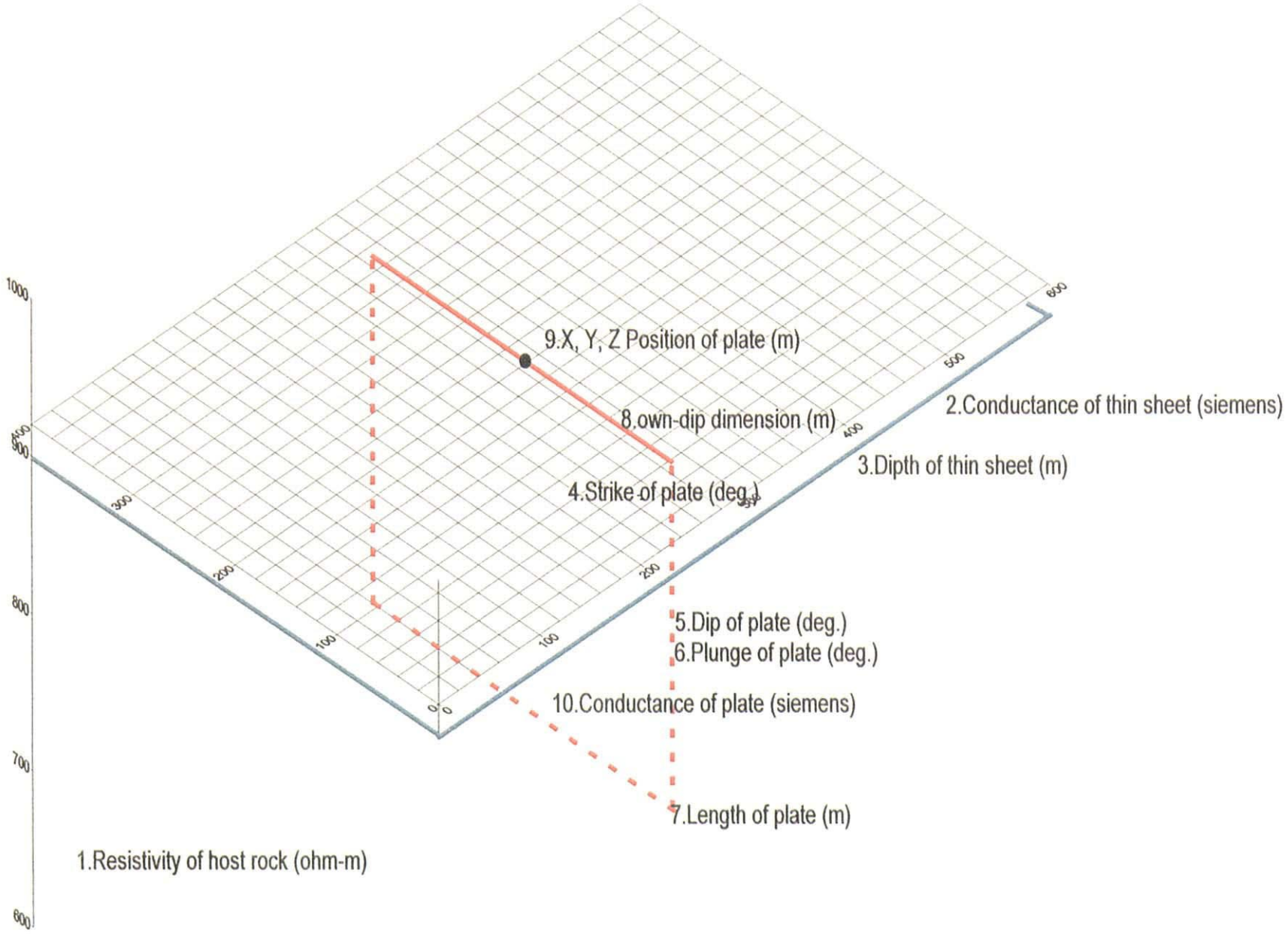

Fig.2-4-3 Parameters of 2D Plate Modeling

(4) Measurements components

Three components (x, y, z) measurement was used to obtain the response by ore body.

The observed voltage profiles at each gate are shown in Figure 2-4-4. The upper profiles show observed voltages of x component, and the lower profiles show those of z component. There can be seen the peak response in each gate around the distance of 100 m in the x component and polarity change in the z component.

The theoretical responses from the two-dimensional plate modeling are shown in Figure 2-4-5. They were calculated using the same loop size of 200 m×400 m as practical measurements. In the case of no conductive plate (a), the voltage changes smoothly from the center of the loop towards the outside of the loop for the x and z components. In a conductive plate model (b), a peak of the x component is seen clearly above the plate model location. For the z component, there is a polarity changing. The position of the polarity change is located the left side of the plate model where is outside of loop source. Since observed voltage profiles show similar feature, it suggests the existence of a conductive plate near the source loop.

In the test field, the previous drilling intersected an ore body. The location of the ore body almost agrees with the position of the conductive plate. Therefore, the conductive plate is probably the ore body. Consequently, the fixed transmitter loop configuration was used for this survey because of the most suitable measurement method to detect the conductive plate-type ore body.

4-3-2 Observed data

TEM survey was carried out in IP anomalous zones extracted by previous IP survey. Five areas were selected as TEM survey areas on the basis of the results of the IP survey and detailed geological survey. The areas were named TB-12, TJ-18, TM-27, TO-21 and TP-18.

The data quality in the field was mostly good, but the signal decreased rapidly and the data from the 11^{th} to 20^{th} gates were in the background noise level because of resistive background medium.
The following descriptions are the results of this survey.

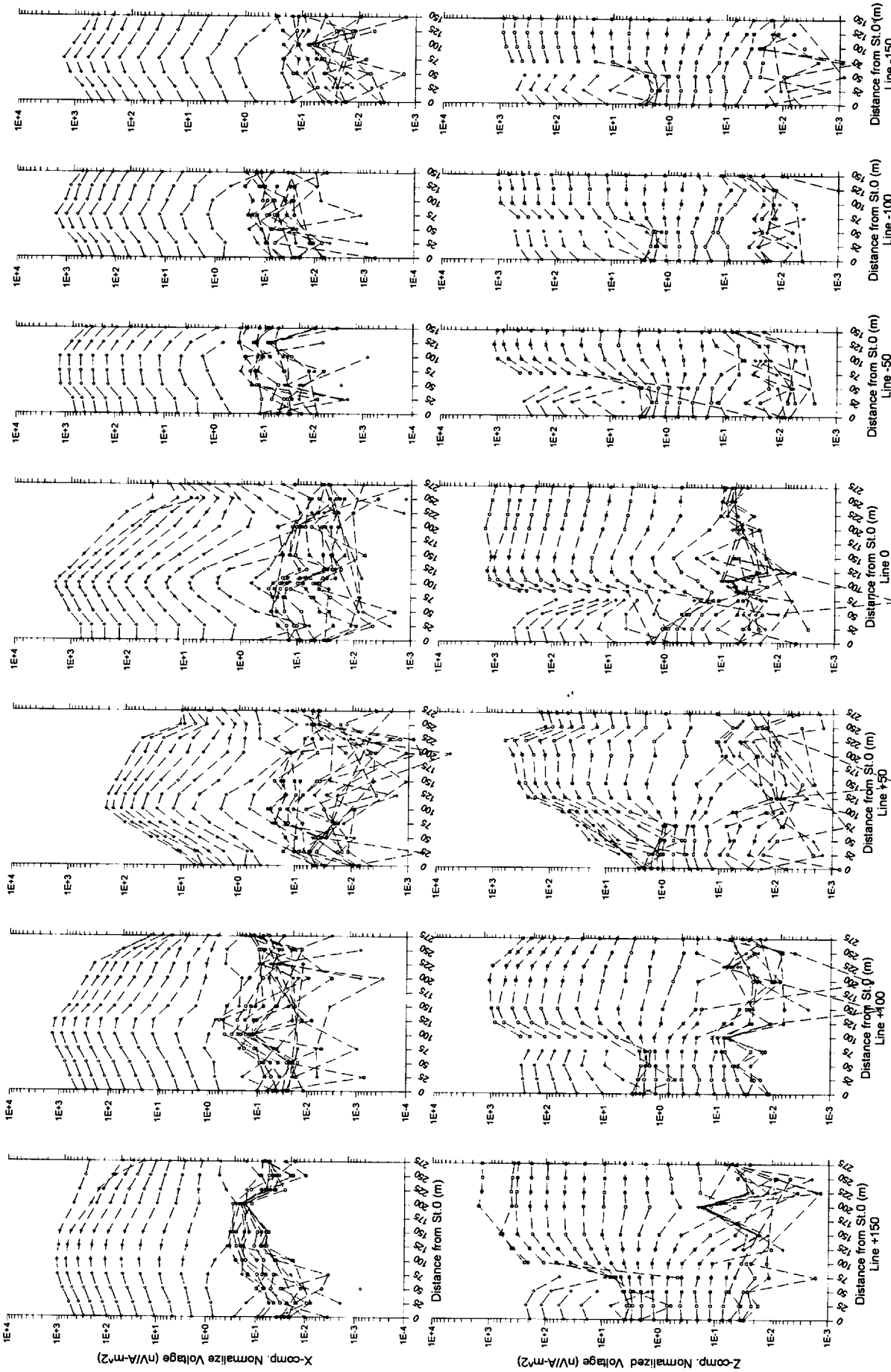

Fig.2-4-4 Observed Voltage Profile of Test Field (TM-8)

*remark;The negative value was changed to positive value

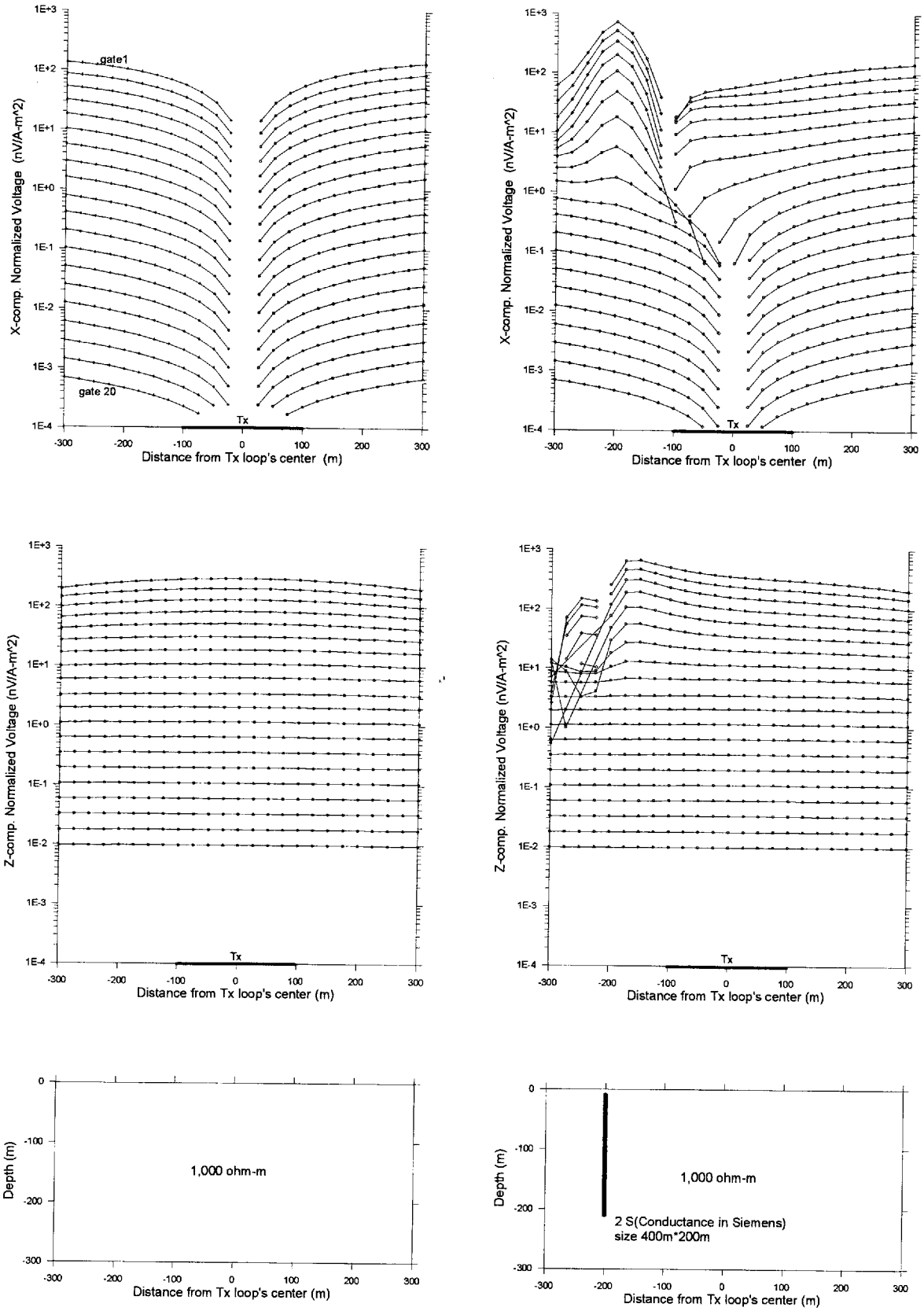

(a) Homogeneous model

(b) Plate model

*remark;The negative value was changed to positive value

positive value negative value

Fig.2-4-5 Theoretical Response for Plate from 2D Plate Modeling

(1) TB-12

This area is located in the northem part of the survey area. It is mainly covered by talus sediment, and dacite is distributed in the west part of the area. The observed voltage profile is shown in the Figure 2-4-6. The profiles of x and z components have same characteristics as the profiles in test measurement area. The peak intensity decreases from Line+150 to Line-150.

The position of conductive plate can be estimated from the peak of x component. The observed voltage distribution map of gate 3 is shown in Figure 2-4-7. The voltage of gate 3 reflects resistivity distribution at shallow depth. There is one ridgeline and its direction is NE-SW.

(2) TJ-18

The area is located around the center of the survey area. There is no outcrop and Quaternary gravel and sand cover the area. The observed voltage profile is shown in Figure 2-4-8. The profiles of x and z components have same characteristics as the profiles in test measurement area. There are some peaks of x component in each profile.

The observed voltage distribution map of gate 3 is shown in Figure 2-4-9. There are three ridgelines on the map. One is in the center of the area and its direction is NE-SW. The other ridgelines are located northwest and southeast, and parallel to the centerline.

(3) TM-27

The area is located in the east part of the survey area. There is no outcrop and Quaternary gravel and sand cover the area. The observed voltage profile is shown in Figure 2-4-10. The profiles of x and z components have same characteristics as the profiles in test measurement area. Two peaks of x component can be seen in both Line+50 and Line+100.

The observed voltage distribution map of gate 3 is shown in Figure 2-4-11. There are two ridgelines on the map. One is in the center of the area and its direction is NE-SW. The other ridgeline passes station No.175 of both Line+100 and Line+150, and its direction is NE-SW.

(4) TO-21

The area is located in the southern part of the survey area. Quaternary gravel and sand with a small amount of tonalite cover the area. The observed voltage profile is shown in Figure 2-4-12. The profiles of x and z components have same characteristics as the profiles in test measurement area.

The observed voltage distribution map of gate 3 is shown in Figure 2-4-13. There is one ridgeline

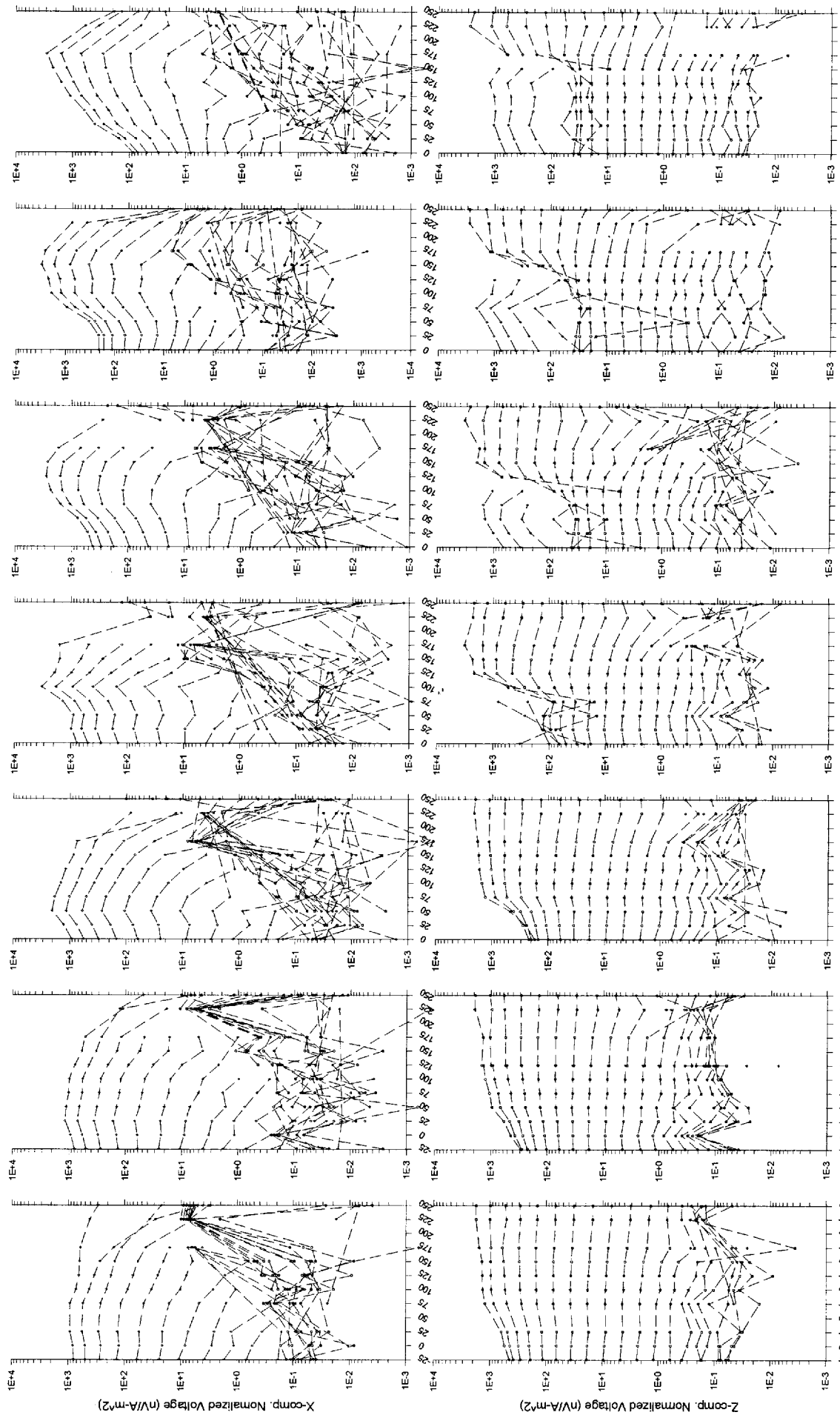

Fig.2-4-6 Observed Voltage Profile (TB-12)

*remark; The negative value was changed to positive value

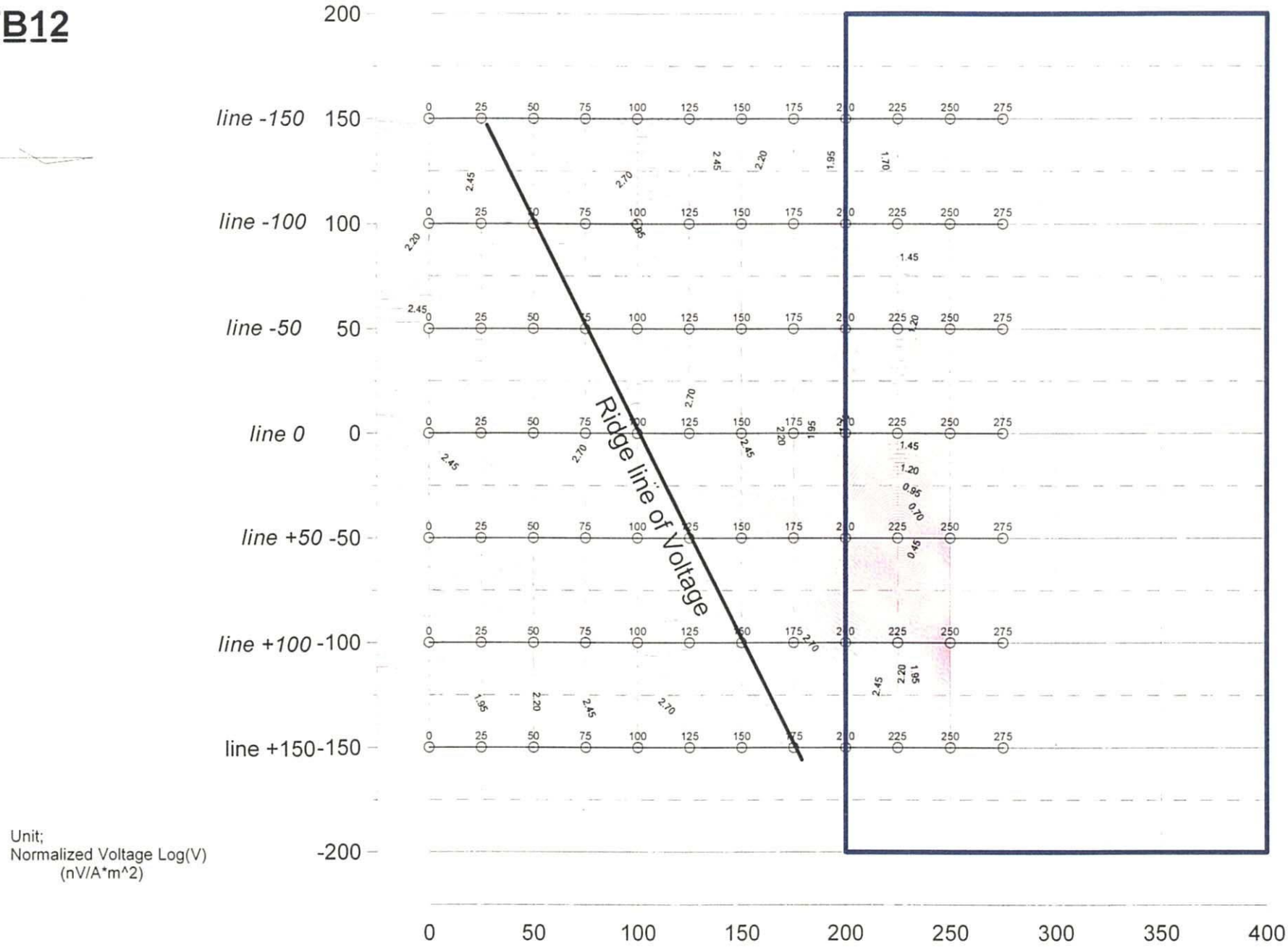

Fig.2-4-7 Observed Voltage Distribution Map of Gate 3 (TB-12)

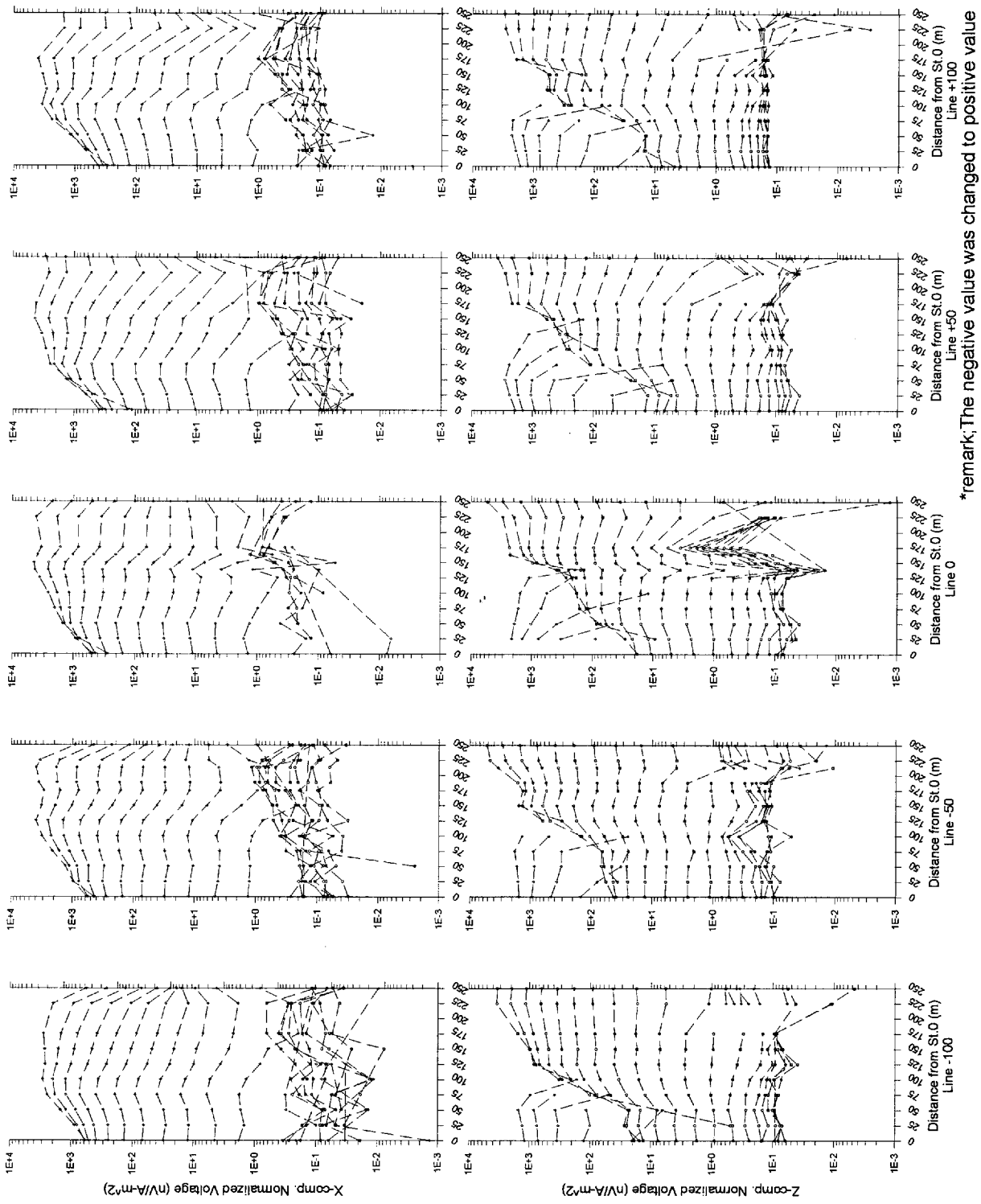

*remark;The negative value was changed to positive value

Fig.2-4-8 Observed Voltage Profile (TJ-18)

TJ18

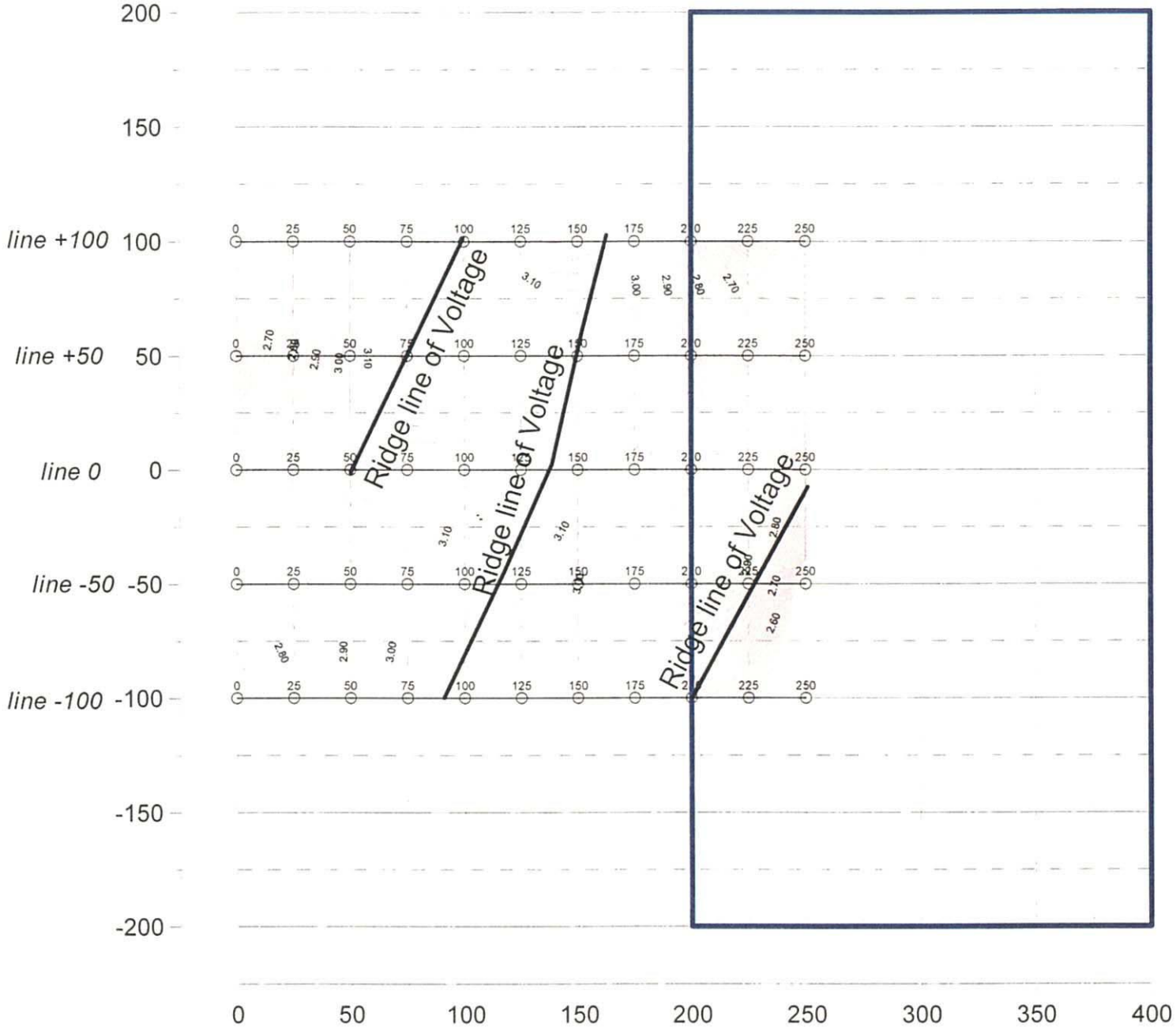

Fig.2-4-9 Observed Voltage Distribution Map of Gate 3 (TJ-18)

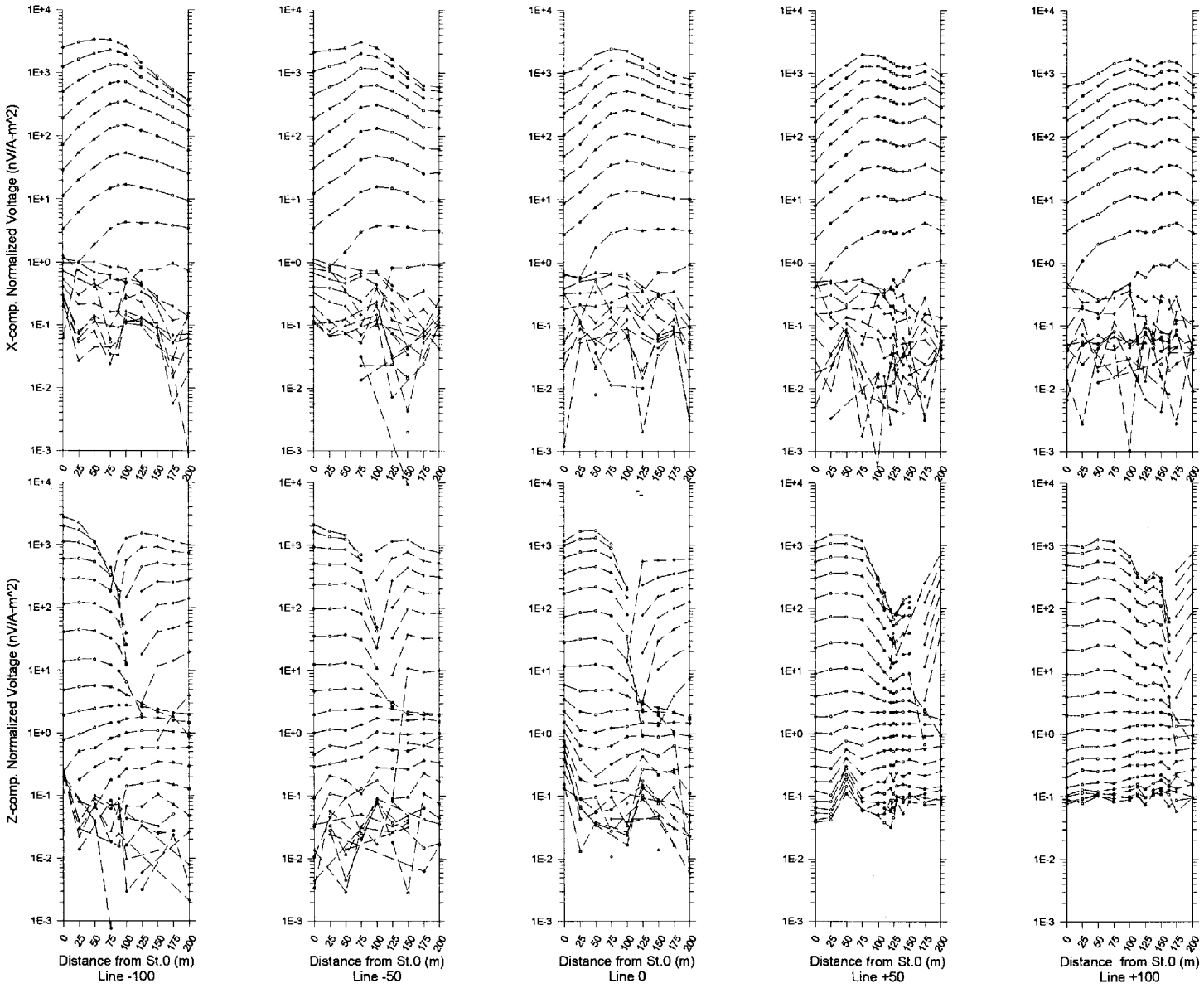

*remark;The negative value was changed to positive value

Fig.2-4-10 Observed Voltage Profile (TM-27)

TM27

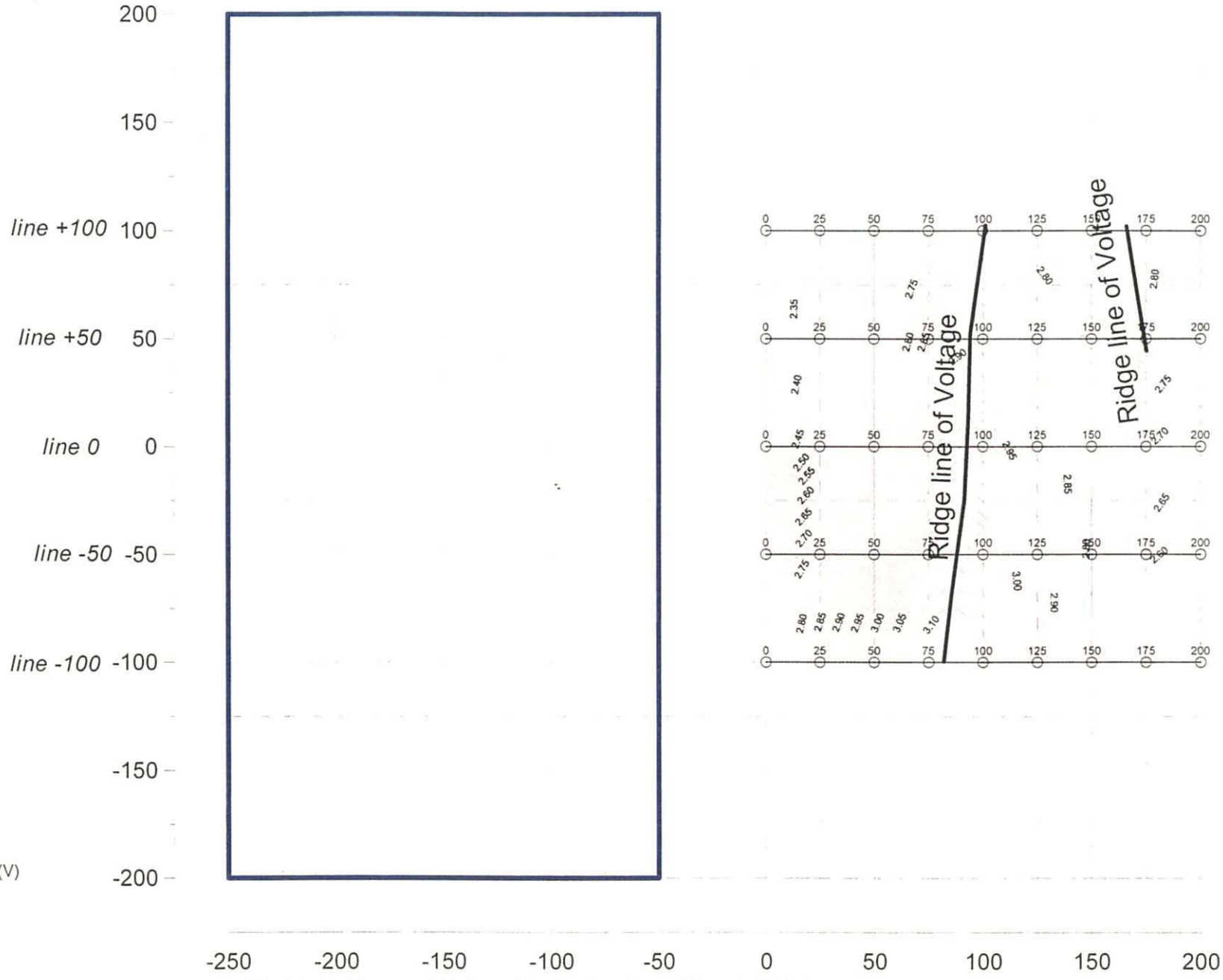

Fig.2-4-11 Observed Voltage Distribution Map of Gate 3 (TM-27)

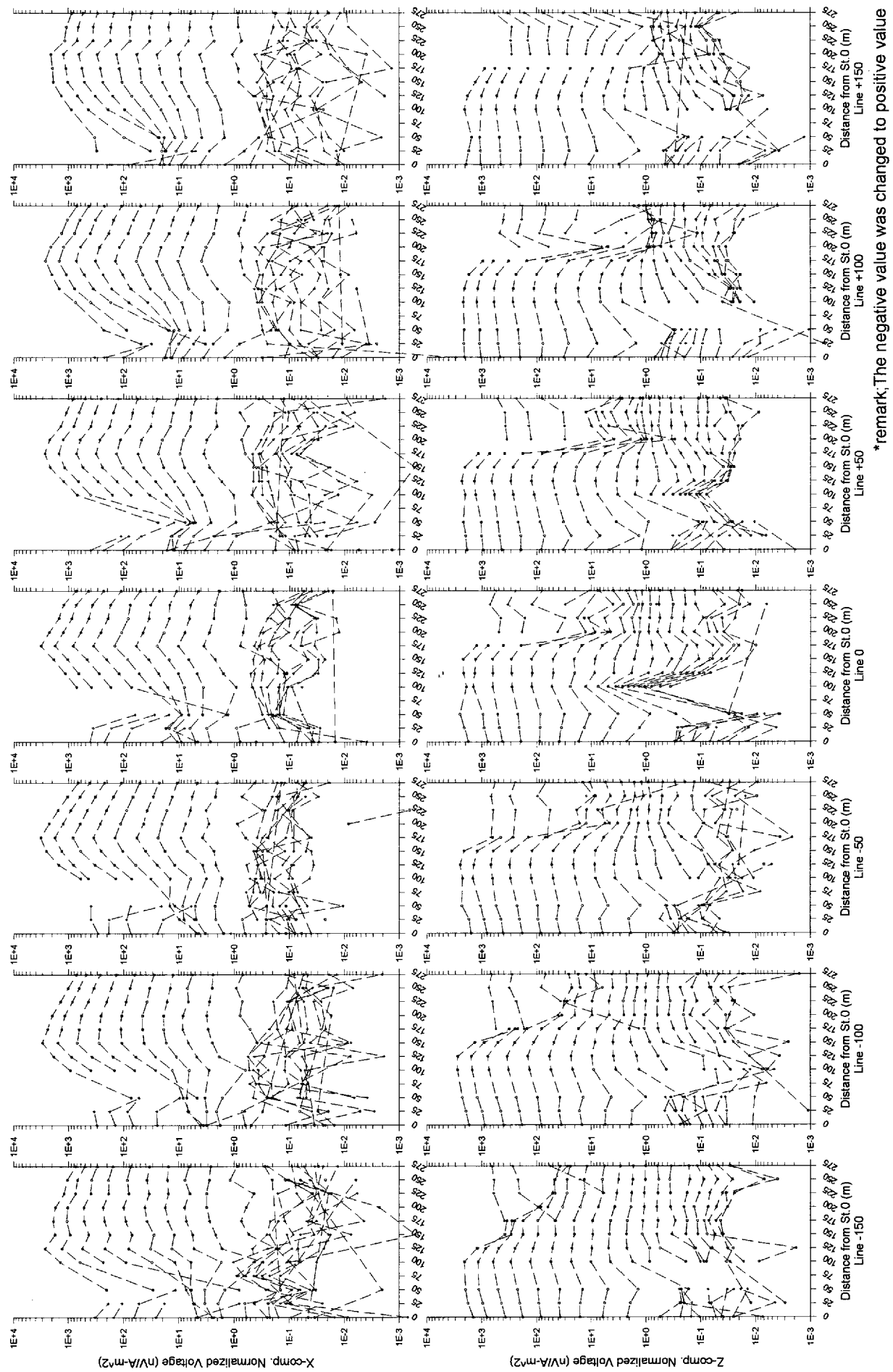

*remark;The negative value was changed to positive value

Fig.2-4-12 Observed Voltage Profile (TO-21)

TO21

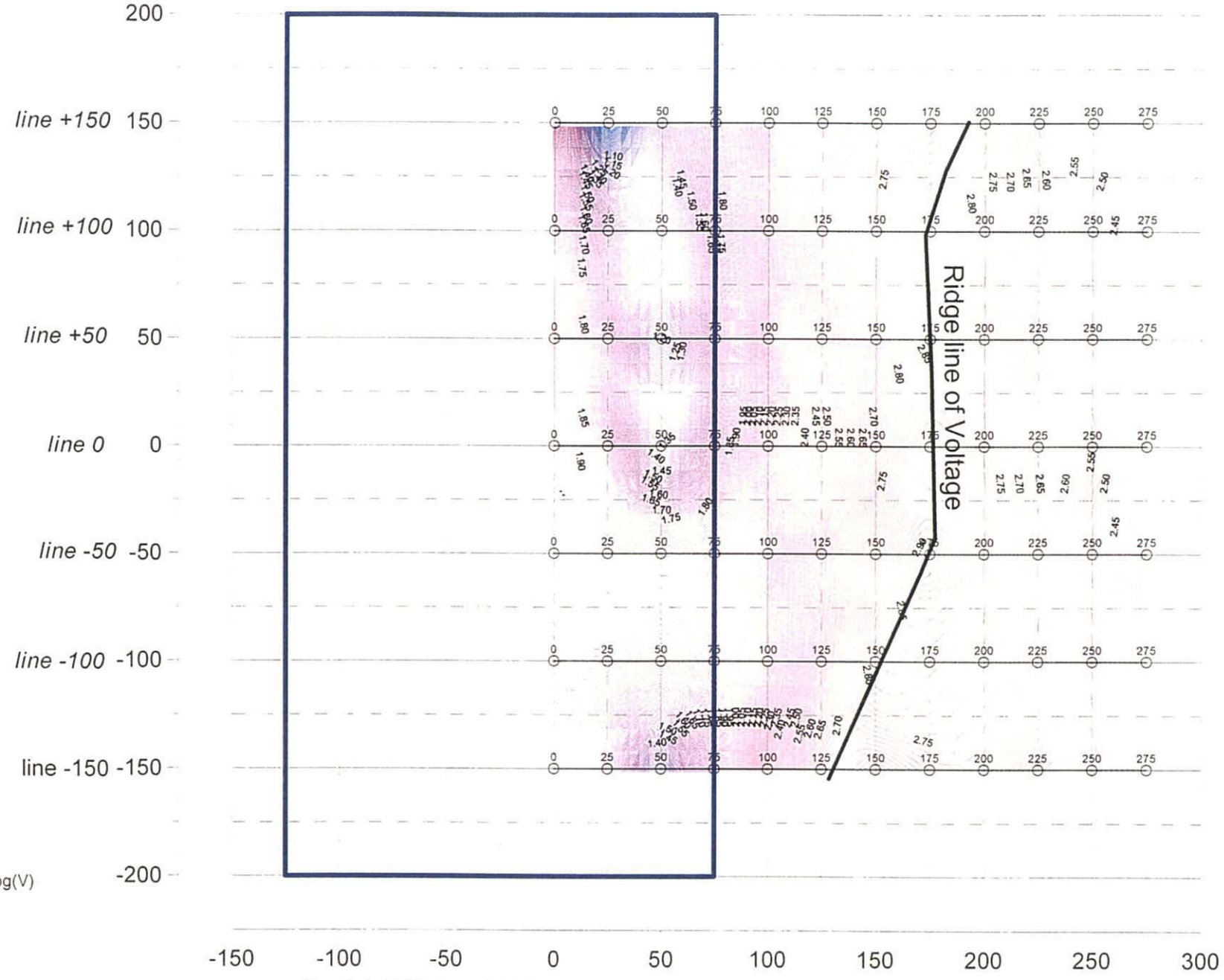

Fig. 2-4-13 Observed Voltage Distribution Map of Gate 3 (TO-21)

on the map. It is in the center of the area and its direction is N-S.

(5) TP-18

The area is located in the southern part of the survey area and near TO-21 area. Quaternary gravel and sand with a small amount of andesite cover the area. The observed voltage profile is shown in Figure 2-4-14. The profiles have lower intensity peaks of x component and no polarity change of z component. It may be caused by smaller difference between the resistivity of plates and that of their surroundings.

The observed voltage distribution map of gate 3 is shown in Figure 2-4-15. There are some small ridgelines on the map.

4-3-3 Analytic results

The results of one-dimensional inversion and two-dimensional plate modeling are the follows.
Data from 1st to 10th gates was used for two-dimensional plate modeling analysis.

(1) TB-12

The resistivity structure section by the one-dimensional inversion is shown in Figure 2-4-16. The resistivity structure has three layers. The resistivity of the second layer is less than several hundreds ohm-m and those of the other layers are more than several thousands ohm-m. The depth of the second layer is 10-100 m and its thickness is several tens of meters.

The estimated plate from two-dimensional plate modeling is shown in Figures 2-4-17. One plate is estimated to extend in the NE-SW direction. The conductance is 1.1 to 2.0 s and the dip of the plate is 80° to the south. The depth of the plate is 300 m from Line+150 to Line+50 and steadily decreases from Line0. At Line-150, the depth is 100 m.

(2) TJ-18

The resistivity structure section by the one-dimensional inversion is shown in Figure 2-4-18. The resistivity structure has two layers. The resistivity of the upper layer is less than 100 ohm-m and that of the lower layer is more than 1,000 ohm-m. The depths of both layers are constant at several tens meters. The upper layer probably shows a weathered zone and the lower layer shows a fresh rock zone.

The estimated plate from two-dimensional plate modeling is shown in Figures 2-4-19. Three plates

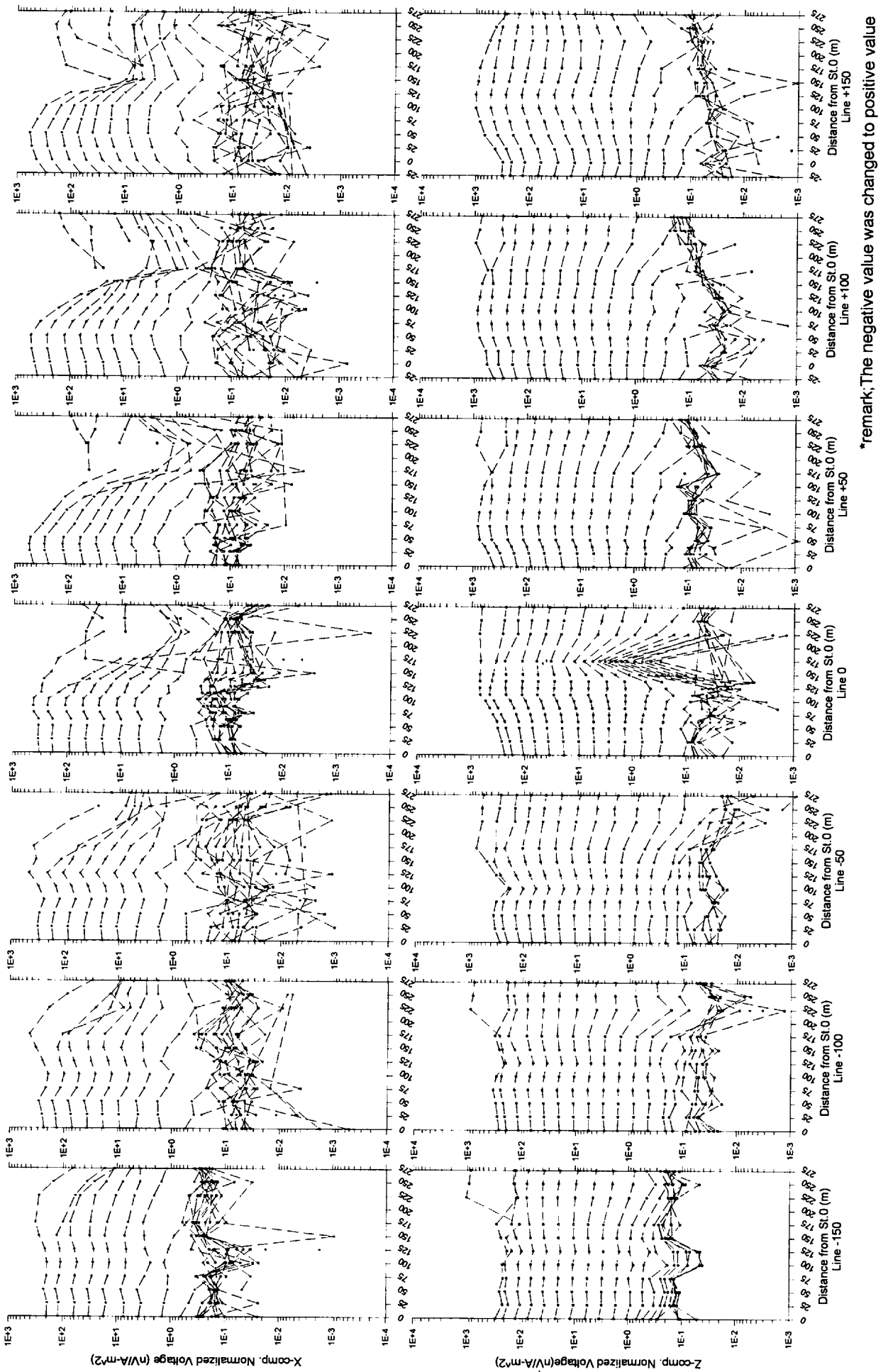

Fig. 2-4-14 Observed Voltage Profile (TP-18)

*remark;The negative value was changed to positive value

TP18

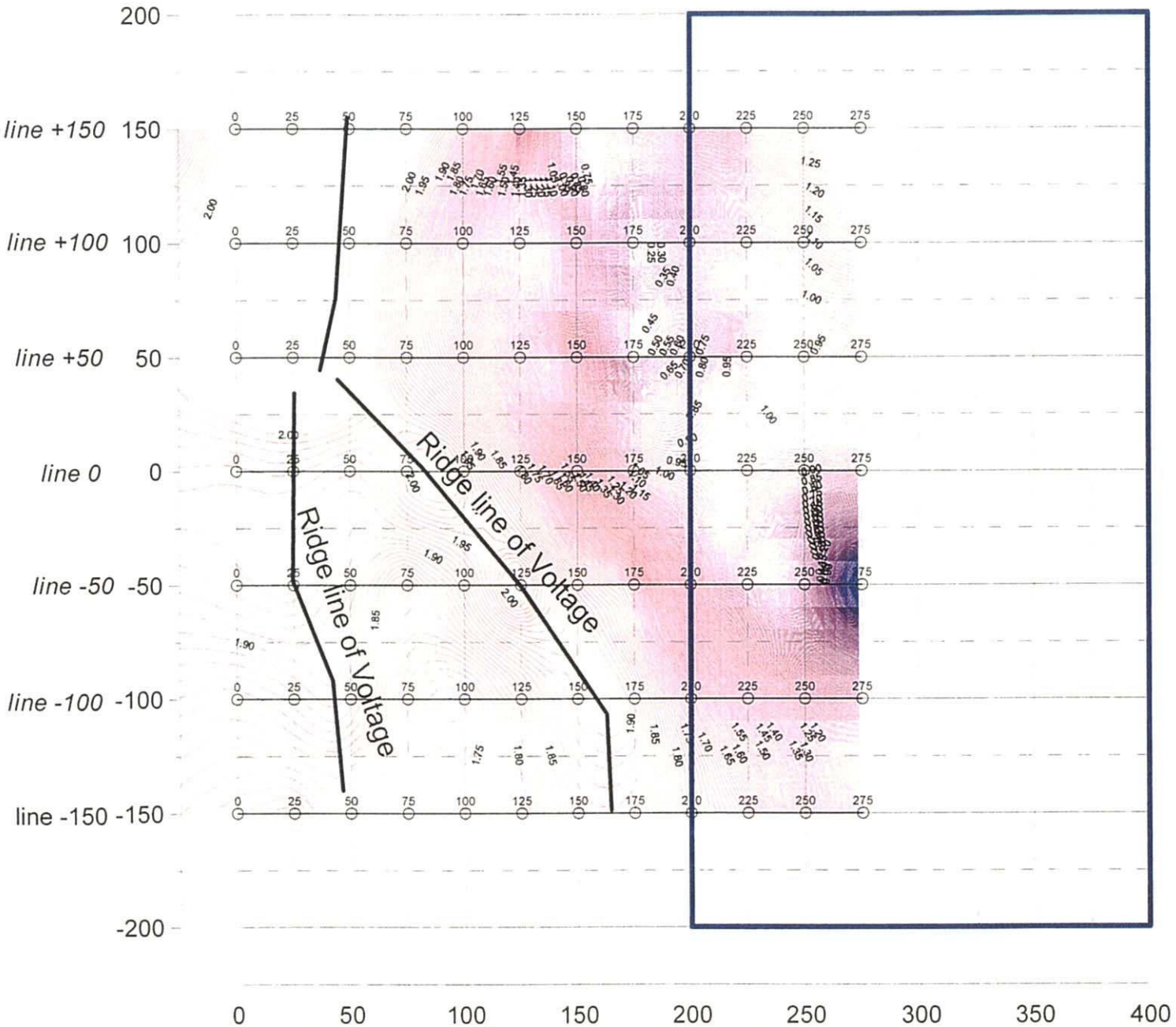

Unit;
Normalized Voltage Log(V)
(nV/A*m^2)

Fig.2-4-15 Observed Voltage Distribution Map of Gate 3 (TP-18)

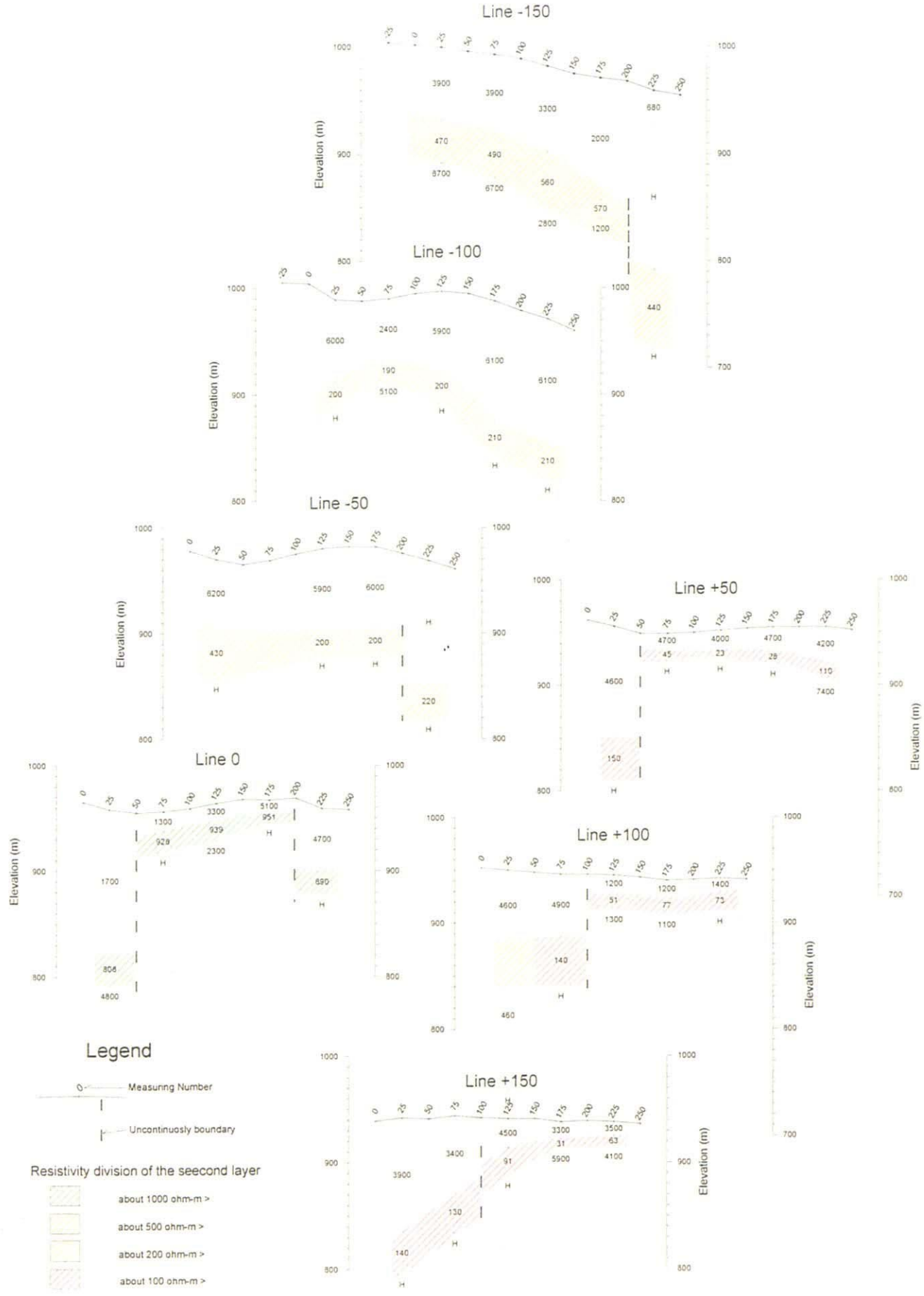

Fig. 2-4-16 Resistivity Structure Section (TB-12)

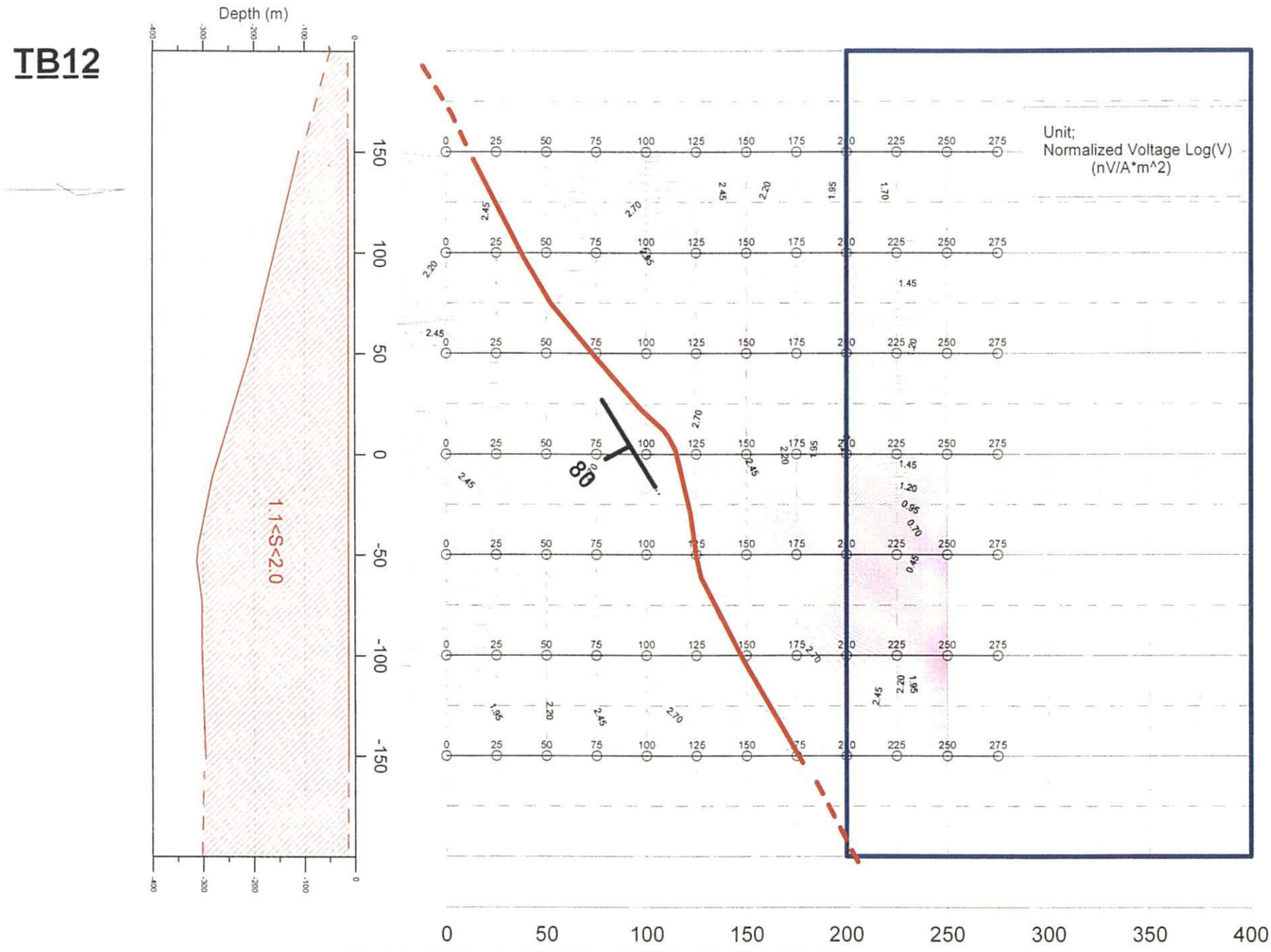

Fig.2-4-17 Estimated Plate from 2D Plate Modeling (TB-12)

Fig. 2-4-18 Resistivity Structure Section (TJ-18)

TJ18

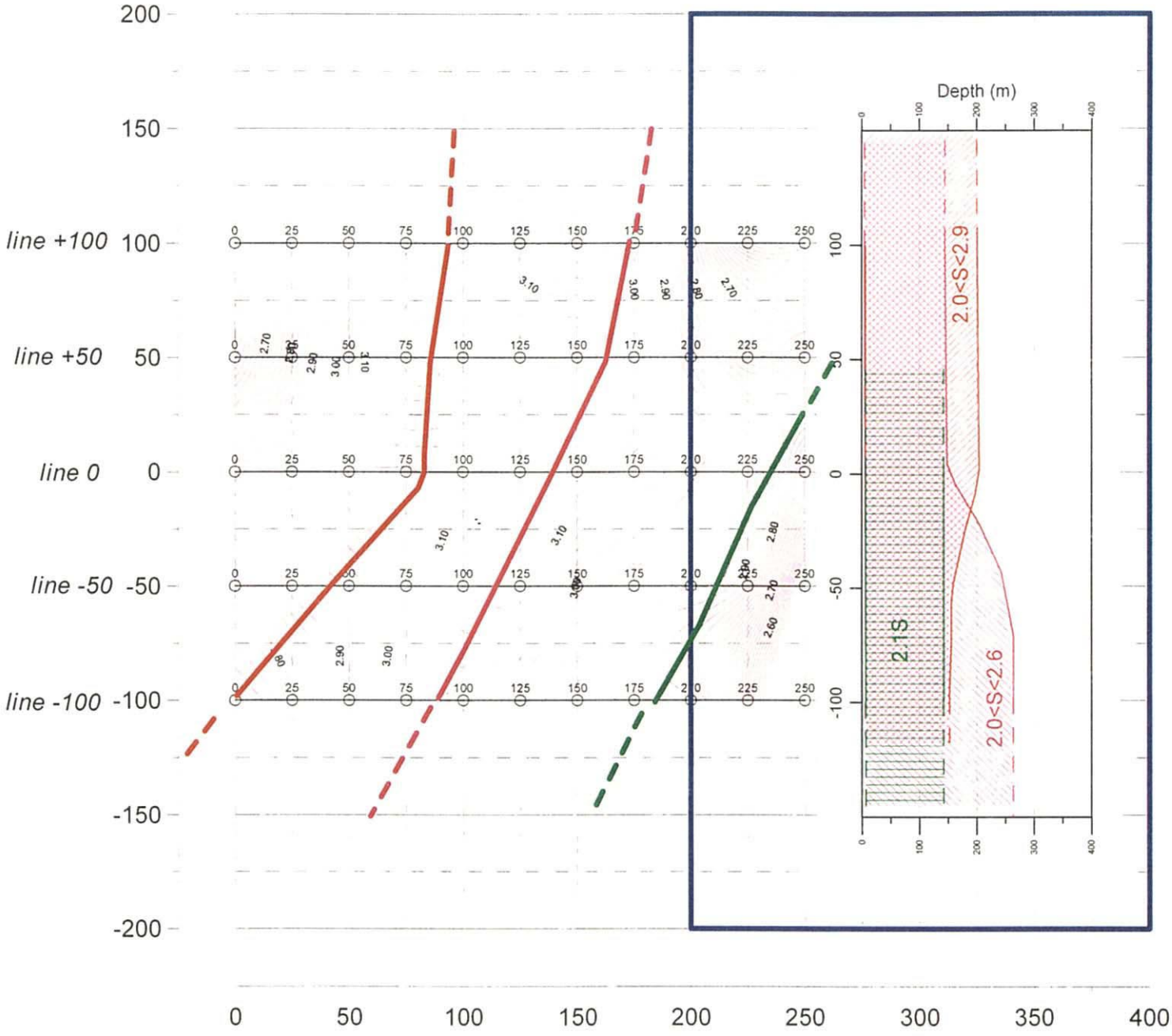

Unit;
Normalized Voltage Log(V)
(nV/A*m^2)

Fig.2-4-19 Estimated Plate from 2D Plate Modeling (TJ-18)

are estimated to be almost parallel to NE-SW. The conductance is 2.0 to 2.9 s and the dip of the plates is 90° . The depth of the central plate is 200-270 m. The depth of NW plate is 150-200 m while the SE plate is constant at 140 m.

(3) TM-27

The resistivity structure section by the one-dimensional inversion is shown in Figure 2-4-20. The resistivity structure has two layers. The resistivity of the upper layer is less than 100 ohm-m and that of the lower layer is more than 1,000 ohm-m. The depths of both layers are constant at several tens meters except for Line+100. The upper layer probably shows a weathered zone and the lower layer shows a fresh rock zone.

The estimated plate from two-dimensional plate modeling is shown in Figure 2-4-21. Two plates are estimated to extend northeastward. The conductance of the central plate is 2.0 to 2.5 s, the dip is 90° , and the depth is constant at 200 m. The conductance of the southern plate is 3.0 s, the dip is 90° , and the depth is constant at 150 m.

(4) TO-21

The resistivity structure section by the one-dimensional inversion is shown in Figure 2-4-22. The resistivity structure has two layers. The resistivity of the upper layer is less than 100 ohm-m and that of the lower layer is more than 1,000 ohm-m. The depths of both layers gradually change from 10 to 40 m with a tendency at station No.75 to be the deepest. The upper layer probably shows a weathered zone and the lower layer shows a fresh rock zone. There is a discontinuous boundary at station No.250 between Line+150 and Line-50.

The estimated plate from two-dimensional plate modeling is shown in Figure 2-4-23. One plate is estimated to pass station No.175 of all survey lines. The conductance of the plate is 1.2 to 1.5 s, the dip of the plate is 90° , and the depth is constant at 270 m.

(5) TP-18

The resistivity structure section by the one-dimensional inversion is shown in Figure 2-4-24. The resistivity structure has two layers. The resistivity of the upper layer is less than 500 ohm-m and that of the lower layer is more than 1,000 ohm-m. The depths of both layers gradually change from 30 to 100 m with a tendency at station No.225 to be the deepest. The upper layer probably shows a weathered zone and the lower layer shows a fresh rock zone.

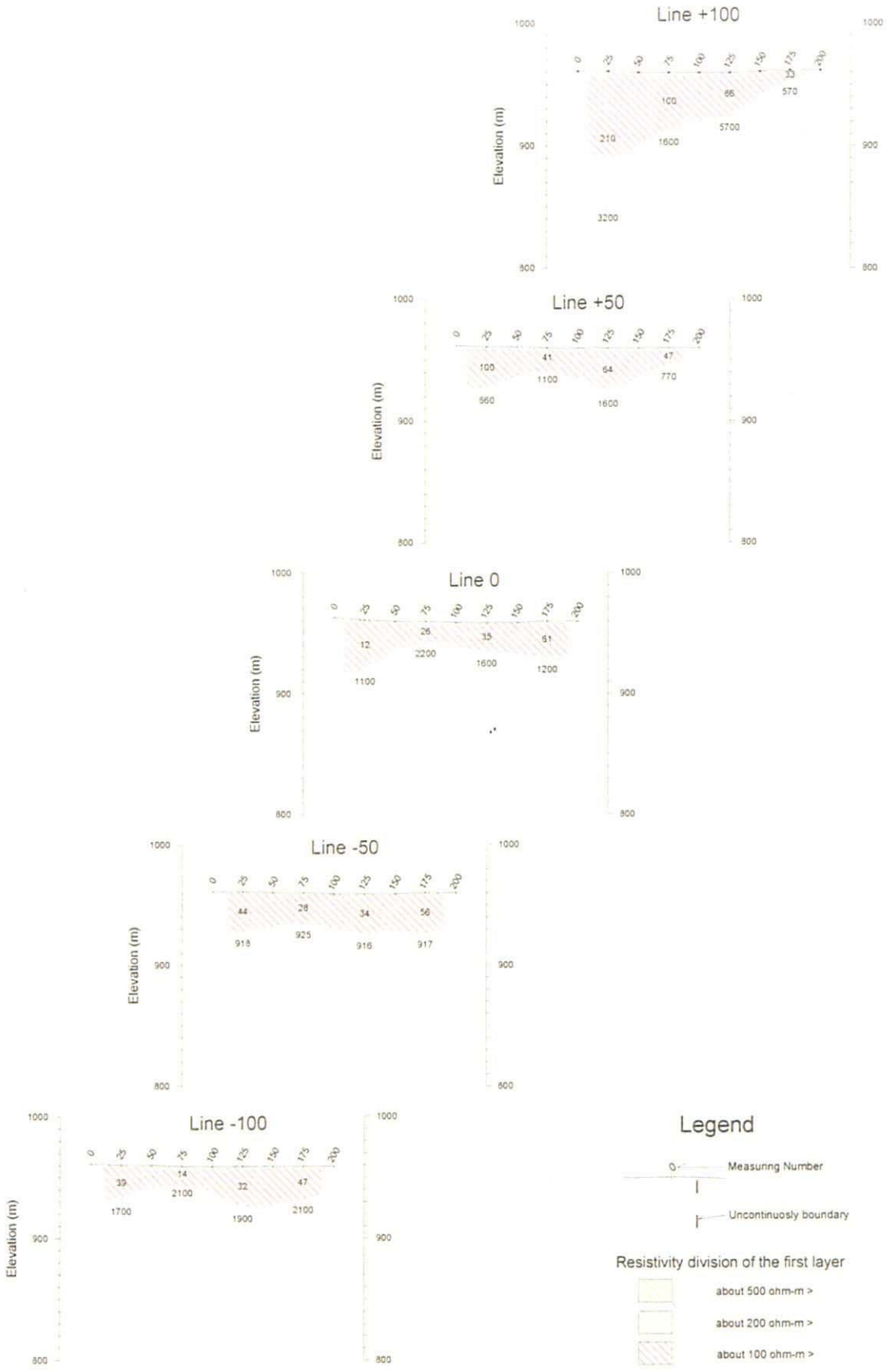

Fig. 2-4-20 Resistivity Structure Section (TM-27)

TM27

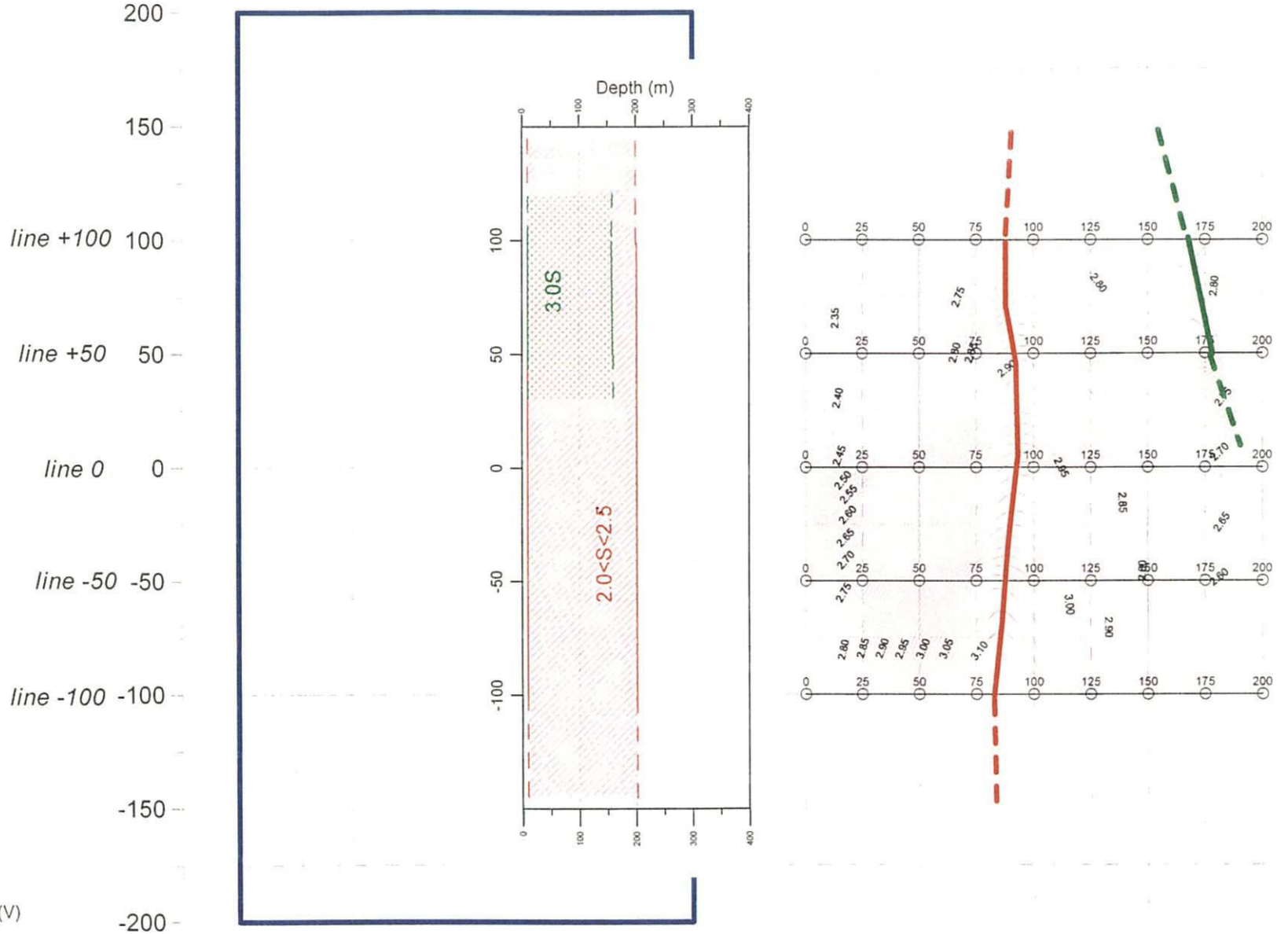

Unit;
Normalized Voltage Log(V)
(nV/A*m^2)

Fig.2-4-21 Estimated Plate from 2D Plate Modeling (TM-27)

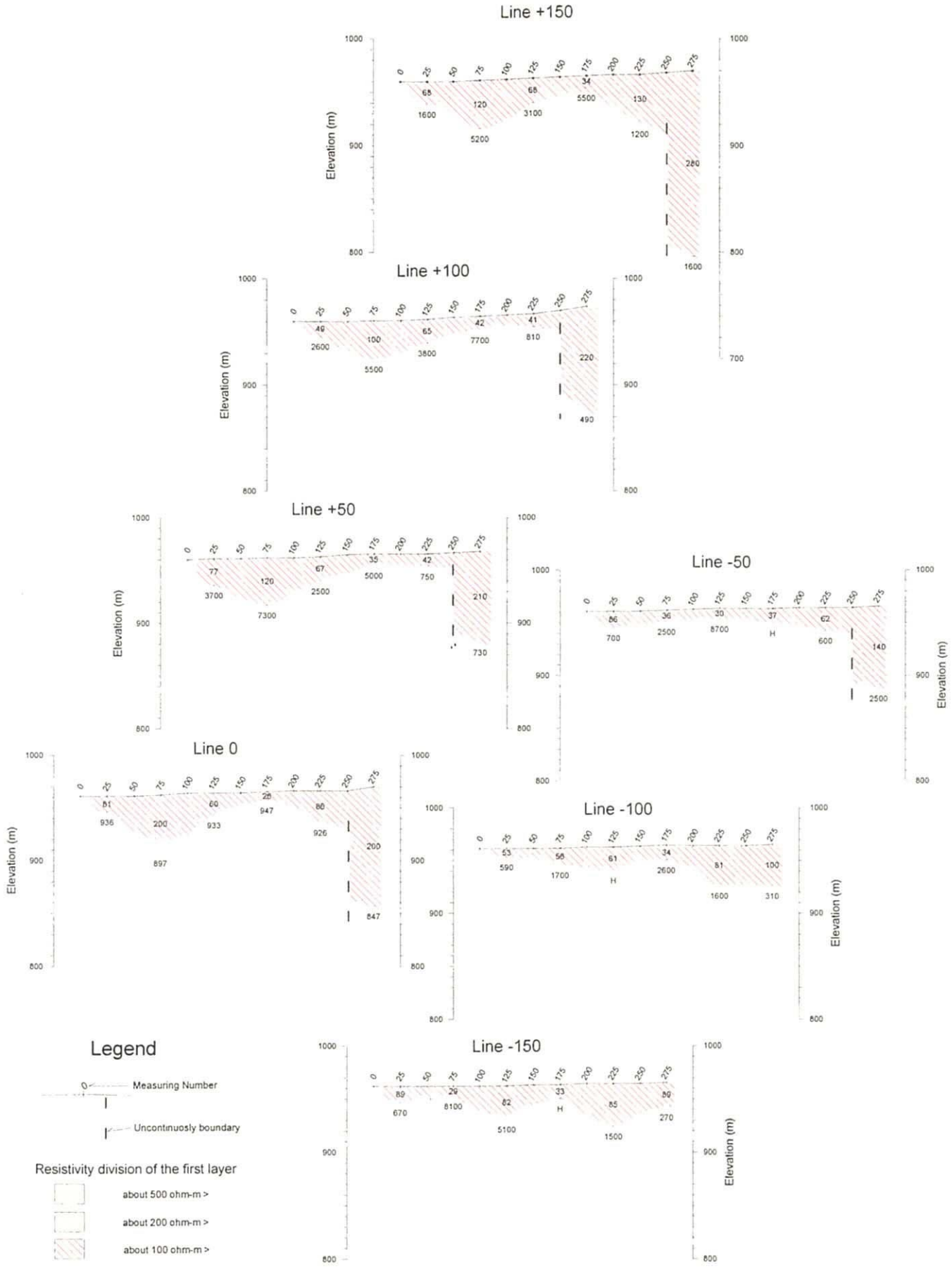

Fig. 2-4-22 Resistivity Structure Section (TO-21)

TO21

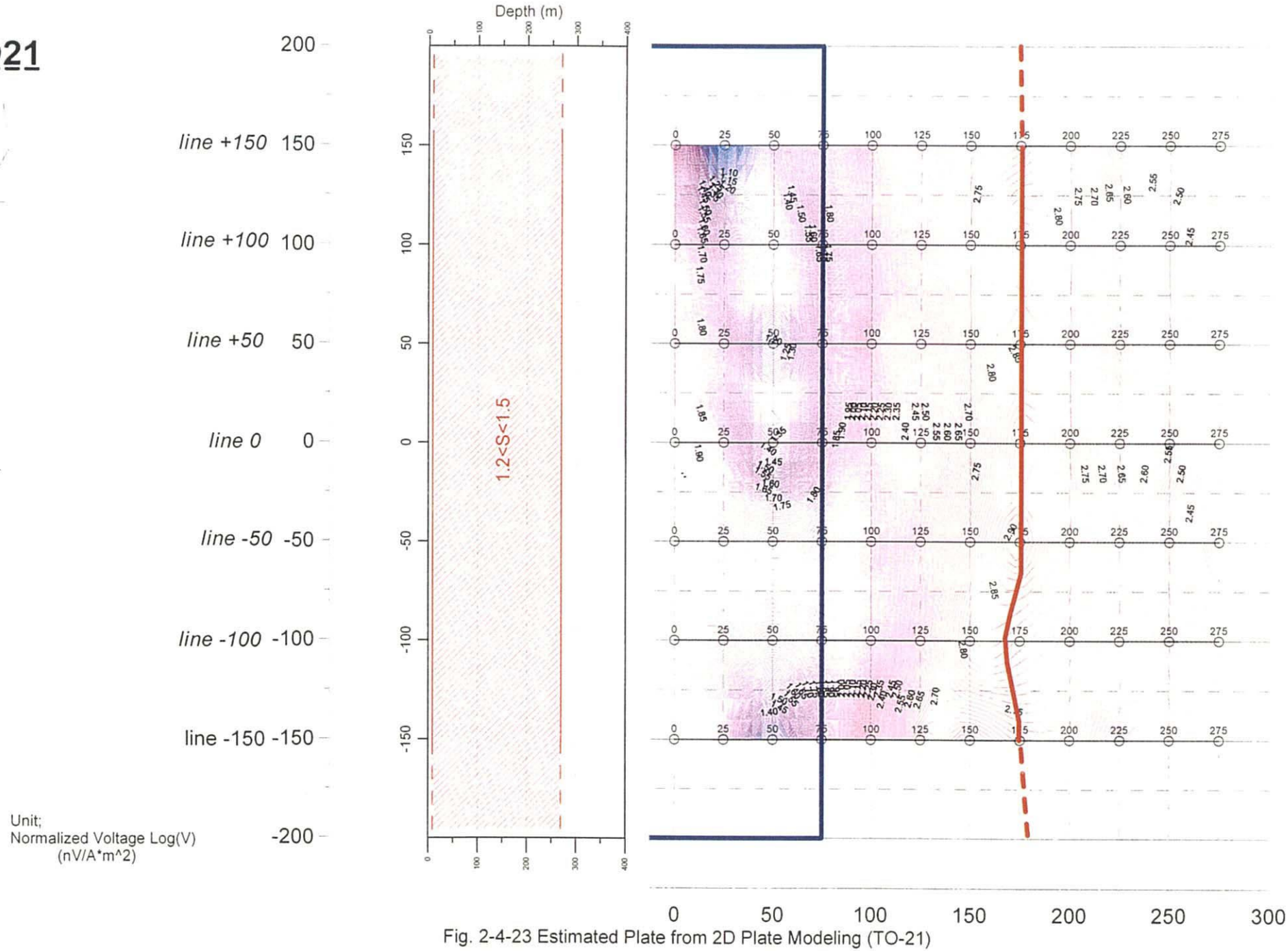

Fig. 2-4-23 Estimated Plate from 2D Plate Modeling (TO-21)

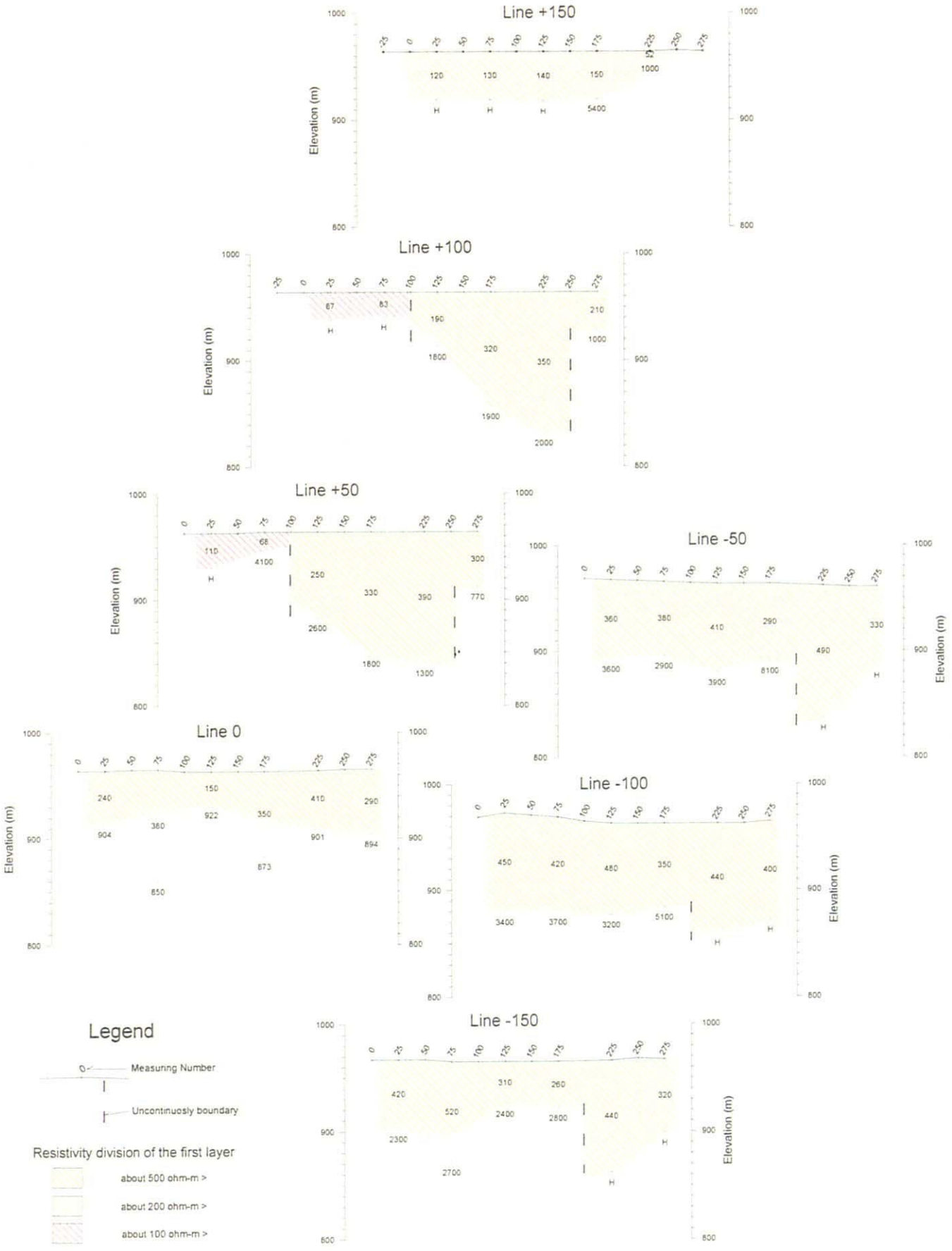

Fig. 2-4-24 Resistivity Structure Section (TP-18)

TP18

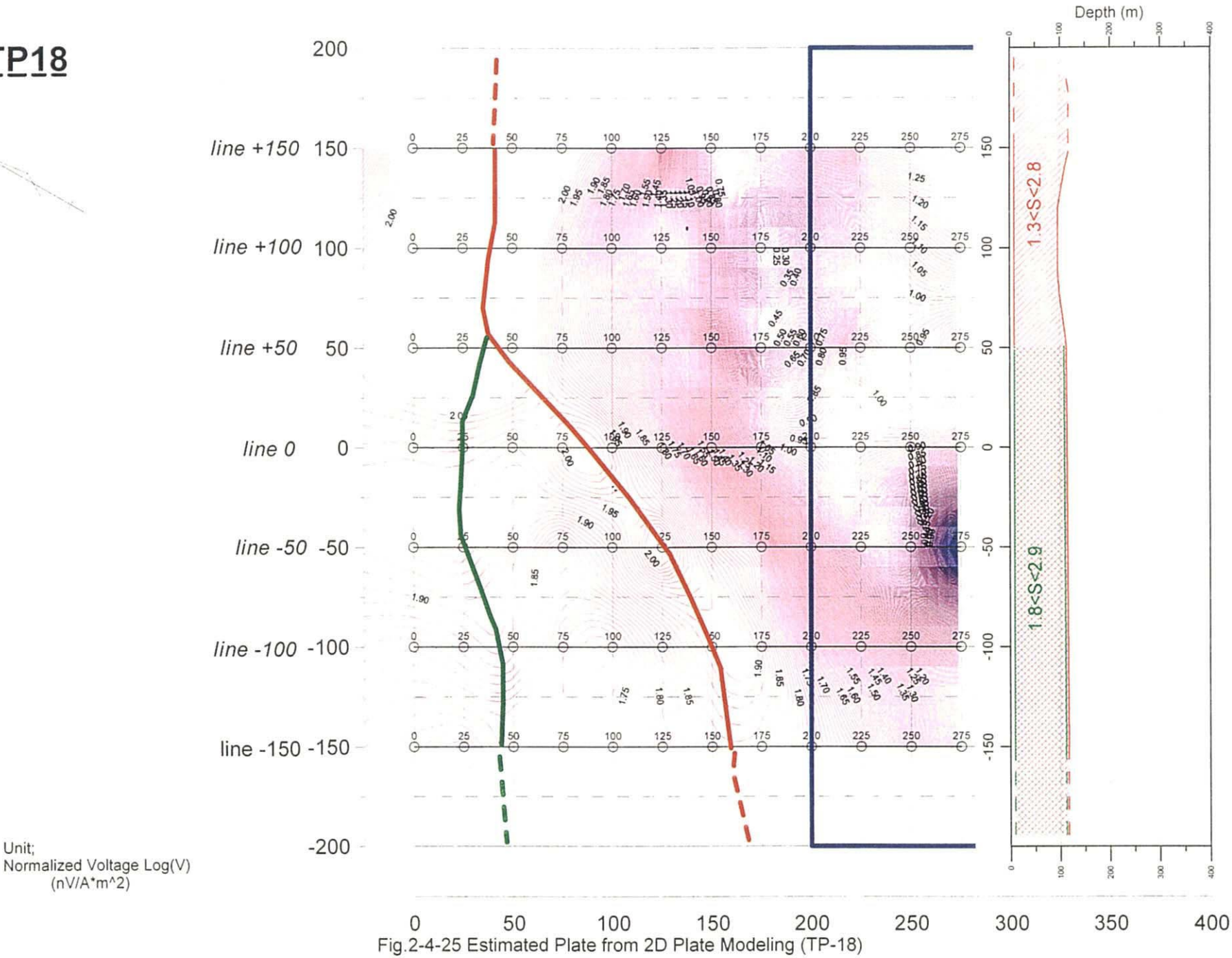

Fig.2-4-25 Estimated Plate from 2D Plate Modeling (TP-18)

The estimated plate from two-dimensional plate modeling is shown in Figure 2-4-25. Two plates are estimated to extend SW-NE, and merge at around station No.50 of Line+50. The conductance of the plates is 1.3 to 2.9 s, the dip is 90° , and the depth is constant at 120 m.

4-3-4 Discussions

TEM survey was carried out on the five IP anomalous zones. Several conductive plates were estimated in each area. The depths of the conductive plates are several hundred meters, the conductance of the plates are from 1 to 3 s and the dips are almost 90° .

In general, a conductive plate shows a fault, groundwater, an alteration zone or a mineralized zone. There are several faults confirmed or estimated in the survey area. These faults were closed and could not contain groundwater because they are Precambrian in age. There is less alteration around mineralized zones according to the drilling survey. Therefore, the conductive plates estimated in this analysis could be mineralized zones.

The ore body intersected by MJSU-2 has 20 ohm-m and 10 m thickness, so the conductance is 0.5 s. The conductance of estimated plates are from 1 to 3 s. This means that the resistivity of estimated mineralized zones will be less than 20 ohm-m and/or the thickness of them will be more than 10 m.

CHAPTER 5 ASSESSMENT

The results of surface geological survey, drilling, examination of existing cores, and IP and TEM geophysical survey are interpreted and mineral potentials of the five sub-areas, where TEM geophysical survey was carried out, are assessed.

5-1 TB-12 Sub-area

Geological map of the sub-area is shown in Figure 2-5-1, and the comprehensive interpretation map in Figure 2-5-2.

IP survey showed very high chargeability values of up to 50mV/V maximum at altitude of 800m (about 150m below the surface). TEM survey resulted in the extraction of NE-SW extending vertical conductive plate and it was named "TB-12A". This plate passes through the maximum chargeability zones. This plate is, from surface survey and drilling results of MJSU-8, inferred to be located within the zone of carbonatized breccia.

The central and eastern parts of this sub-area is covered by talus deposits from Jabal Sujarah (Mt. Sujarah). It is confirmed by MJSU-8 that breccia and tuff of Arj Group occur below these talus deposits. Also dacite and carbonatized breccia are exposed in the western part of this sub-area. In MJSU-8, chalcopyrite and sphalerite breccia ores were found at 73.25—73.55m depth and also pyrite-chalcopyrite massive ore at 82.65—83.35m depth. But the amount of pyrite decreased in the deeper zones and the drilling was ceased at 250.00m depth. Results of TEM survey was obtained after completion of the drilling and the extracted plate occur 30m north of the bottom of MJSU-8. Thus the possibility of the existence of a mineralized zone different form those confirmed by MJSU-8 is high. Further drilling is necessary for comprehensive assessment of mineralization of this sub-area.

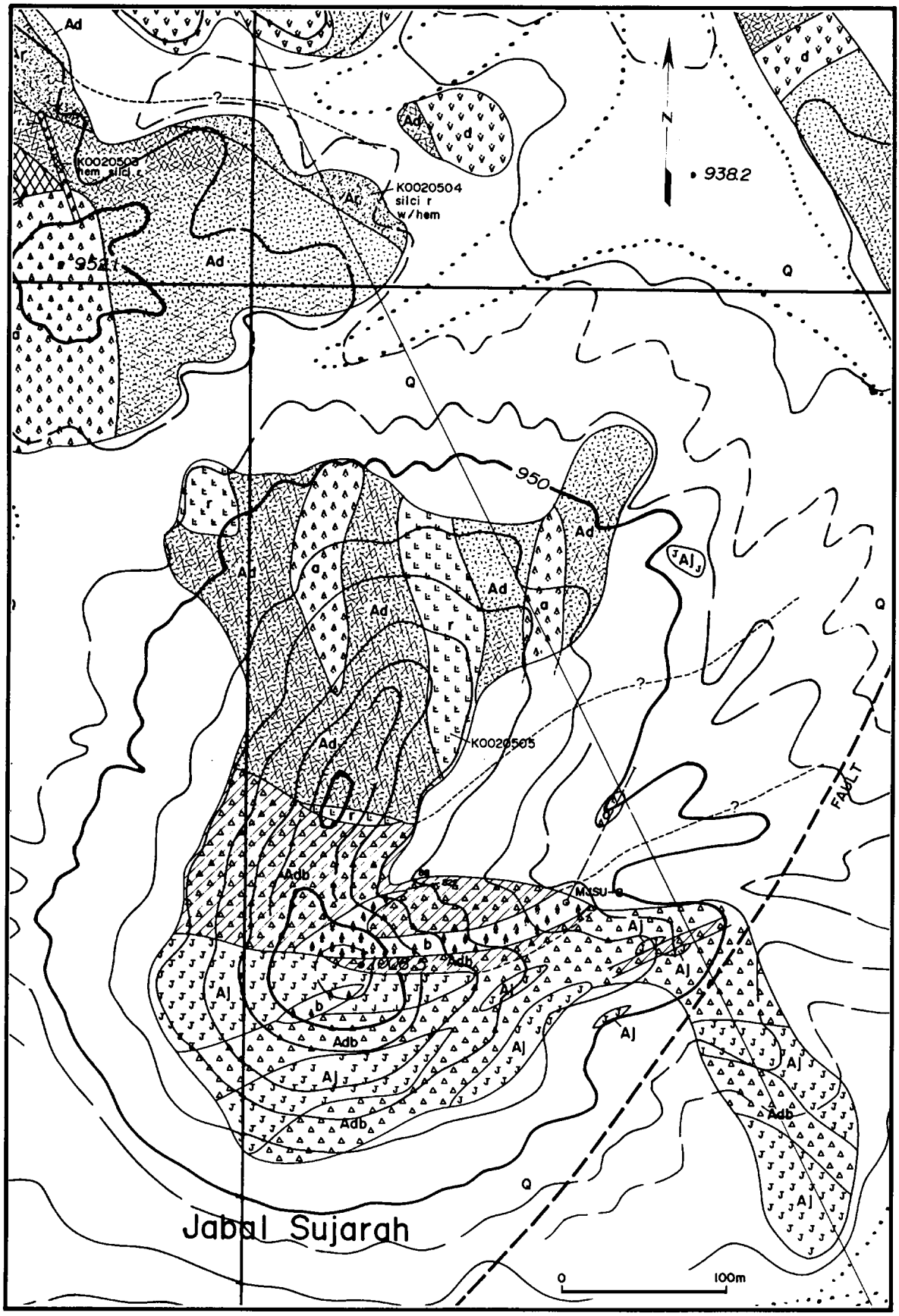

Fig.2-5-1 Detailed Geological Map of TB-12

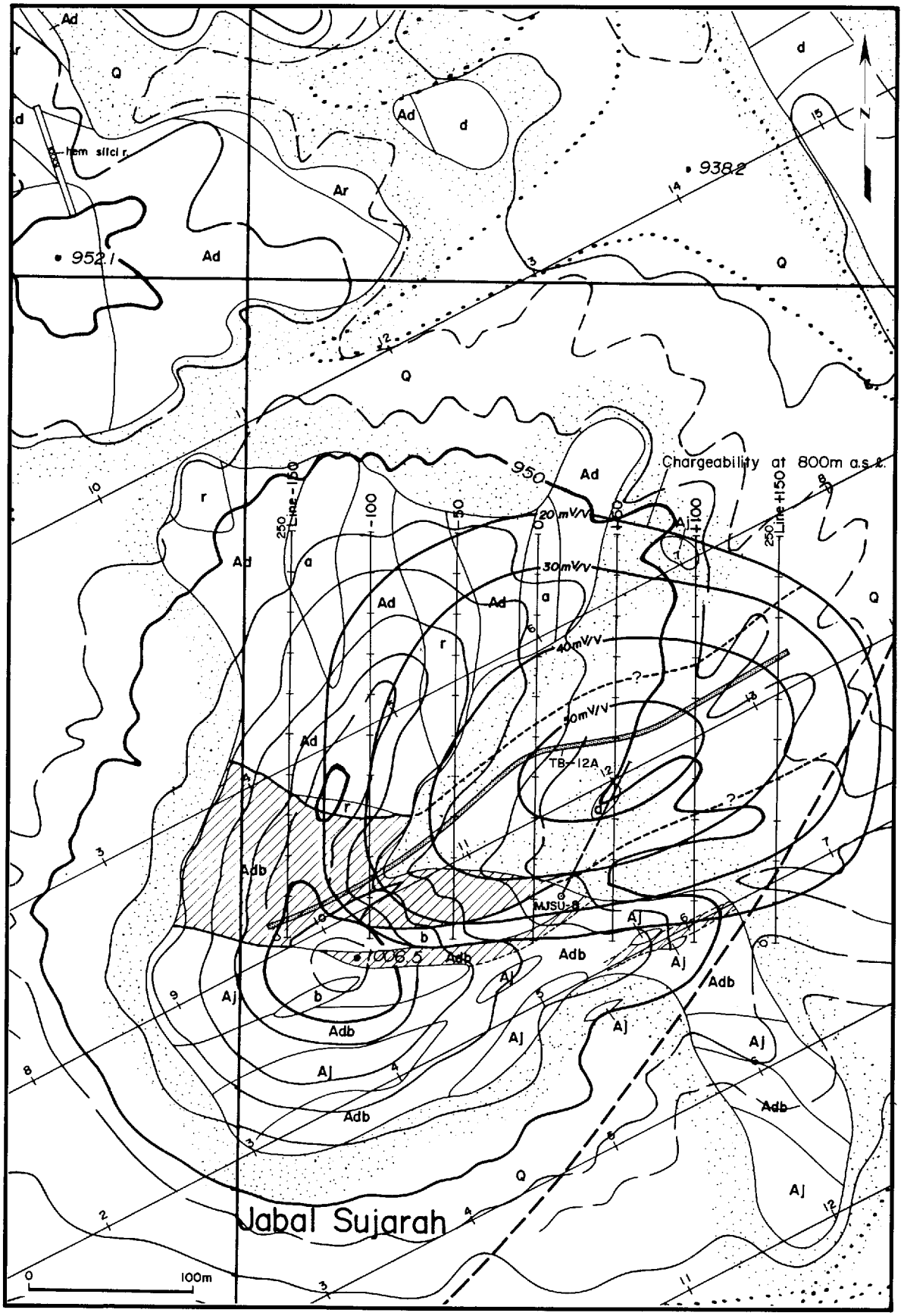

Fig.2-5-2 Integrated Interpretation Map of TB-12

5-2 TJ-18 Sub-area

Geological map of the sub-area is shown in Figure 2-5-3, and the comprehensive interpretation map in Figure 2-5-4.

IP survey showed the highest chargeability values of exceeding 21mV/V at altitude of 800m (about 150m below the surface) near station 18 of IP traverse 98J. TEM survey resulted in the extraction of three NE-SW extending vertical conductive plates and they were named "TJ-18B", "TJ-18A", and "TJ-18C" from the west eastward. TJ-18A passes near the above Station 18.

There is a small ancient pit near TJ-18A and hematitized rhyodacite is observed. UAD-7 and UAD-10 holes drilled by SEREM/US Steel in 1977 are located 300m east of this pit. The cores of UAD-10 show that the geology of this hole consists of rhyodacitic pyroclastic rocks. And these rocks probably are distributed in this sub-area. Occurrence of volcanogenic massive sulfide-type Cu-Zn mineralization is highly possible in TJ-18.

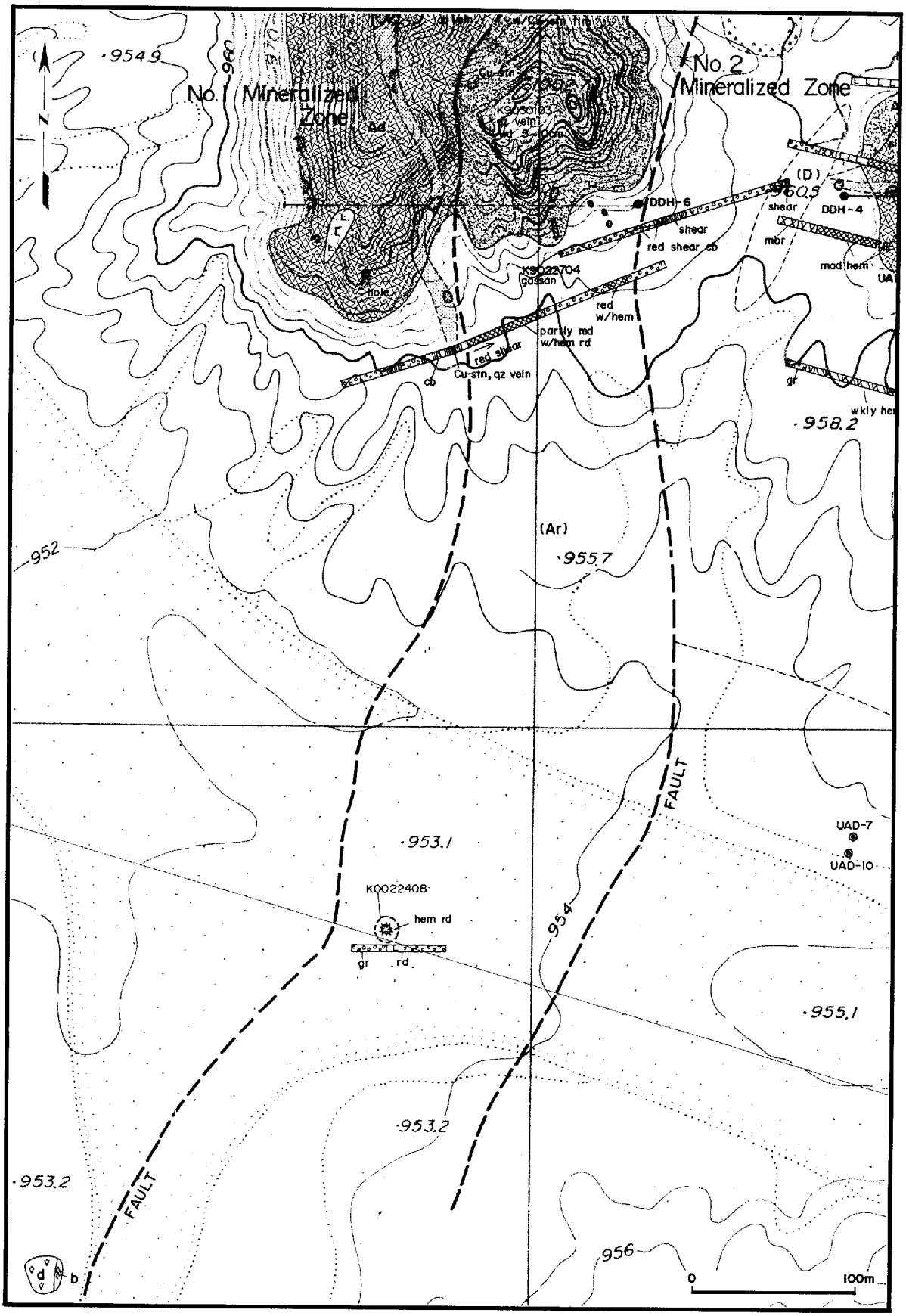

Fig.2-5-3 Detailed Geological Map of TJ-18

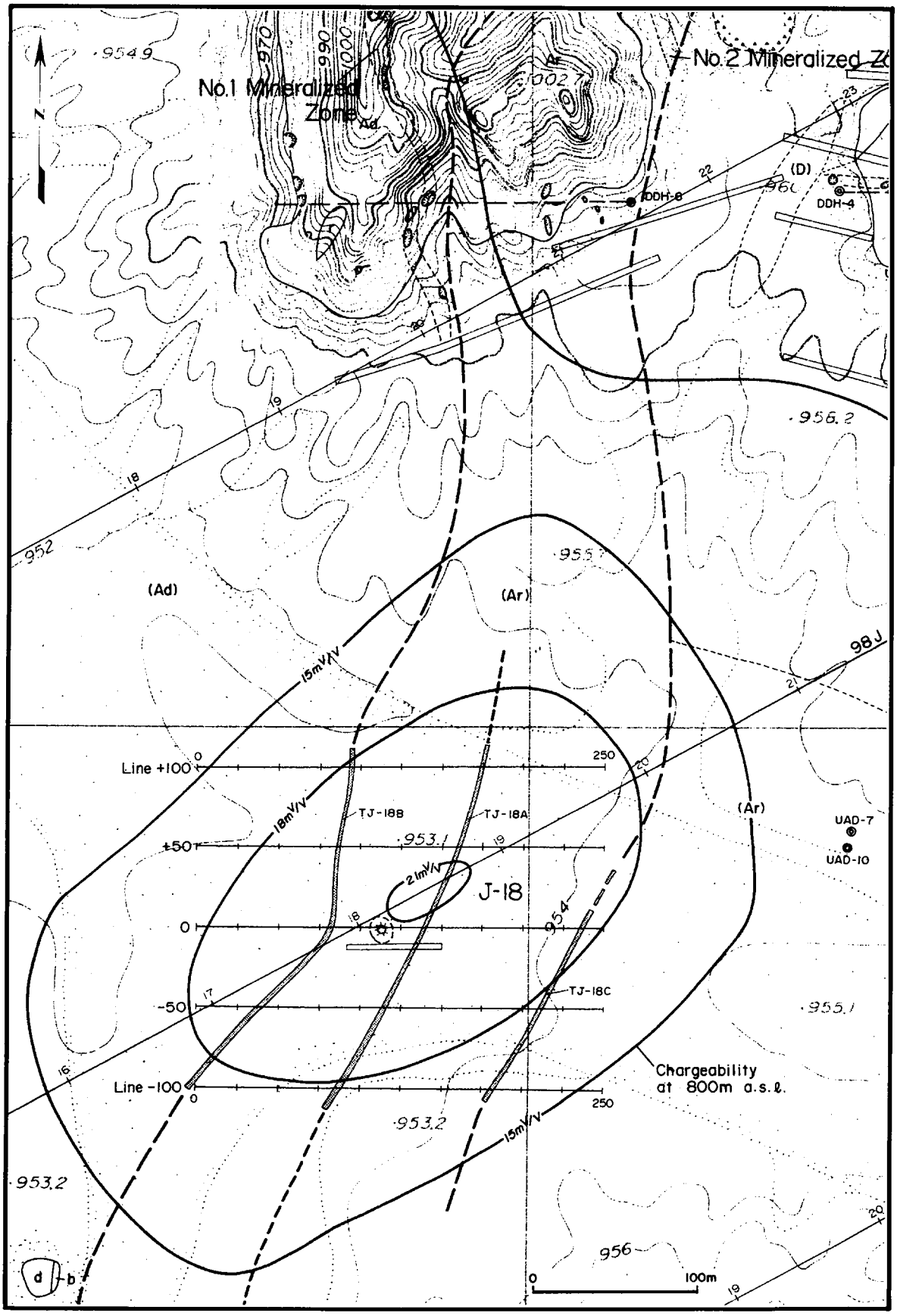

Fig.2-5-4 Integrated Interpretation Map of TJ-18

5-3 TM-27 Sub-area

Geological map of the sub-area is shown in Figure 2-5-5, and the comprehensive interpretation map in Figure 2-5-6.

IP survey showed the highest chargeability values exceeding 24mV/V at altitude of 800m (about 150m below the surface) from station 26 to 28 of IP traverse 98M. TEM survey resulted in the extraction of two NE-SW extending vertical conductive plates and the northern plate was named "TM-27A" and the southern one "TM-27B". TM-27A is located at the central part of chargeability anomaly.

The subsurface geology of this sub-area is not clear because the TEM traverse lines are mainly over Quaternary sand and gravel bed. It is inferred, however, from the surface geology near the traverse lines that dacite, dacitic pyroclastic rocks, and porphyritic andesite (intrusive body) occur in subsurface zones. Drilling has not been carried out in this sub-area in the past. Copper oxide dissemination is observed at the boundary between dacite and jasper of the Arj Group and two small ancient pits occur near station 7 of IP traverse 99D.

Rhyodacitic pyroclastic rocks do not occur at the periphery of this sub-area, and the TM-27A is inferred to reflect vein-type mineralization.

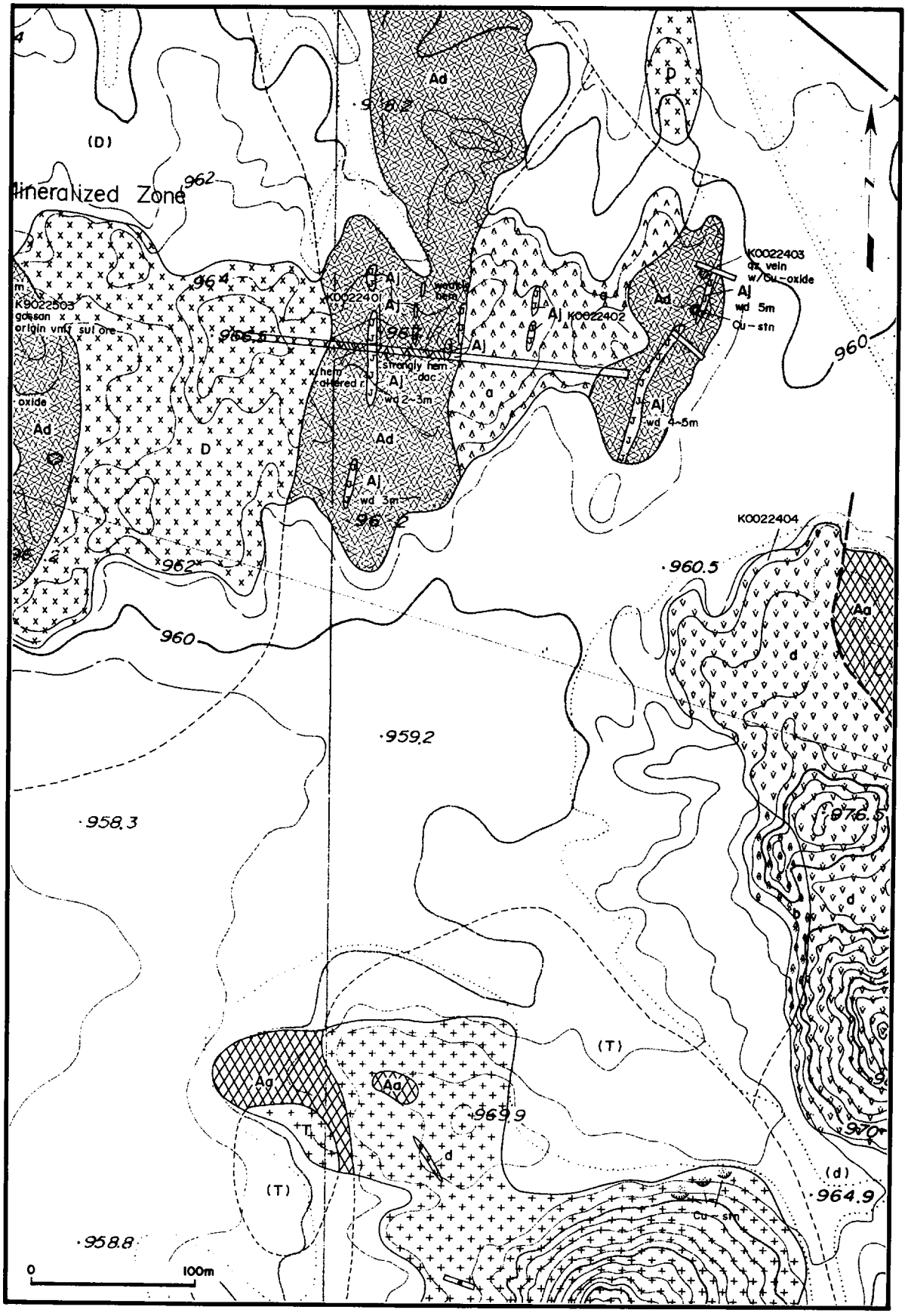

Fig.2-5-5 Detailed Geological Map of TM-27

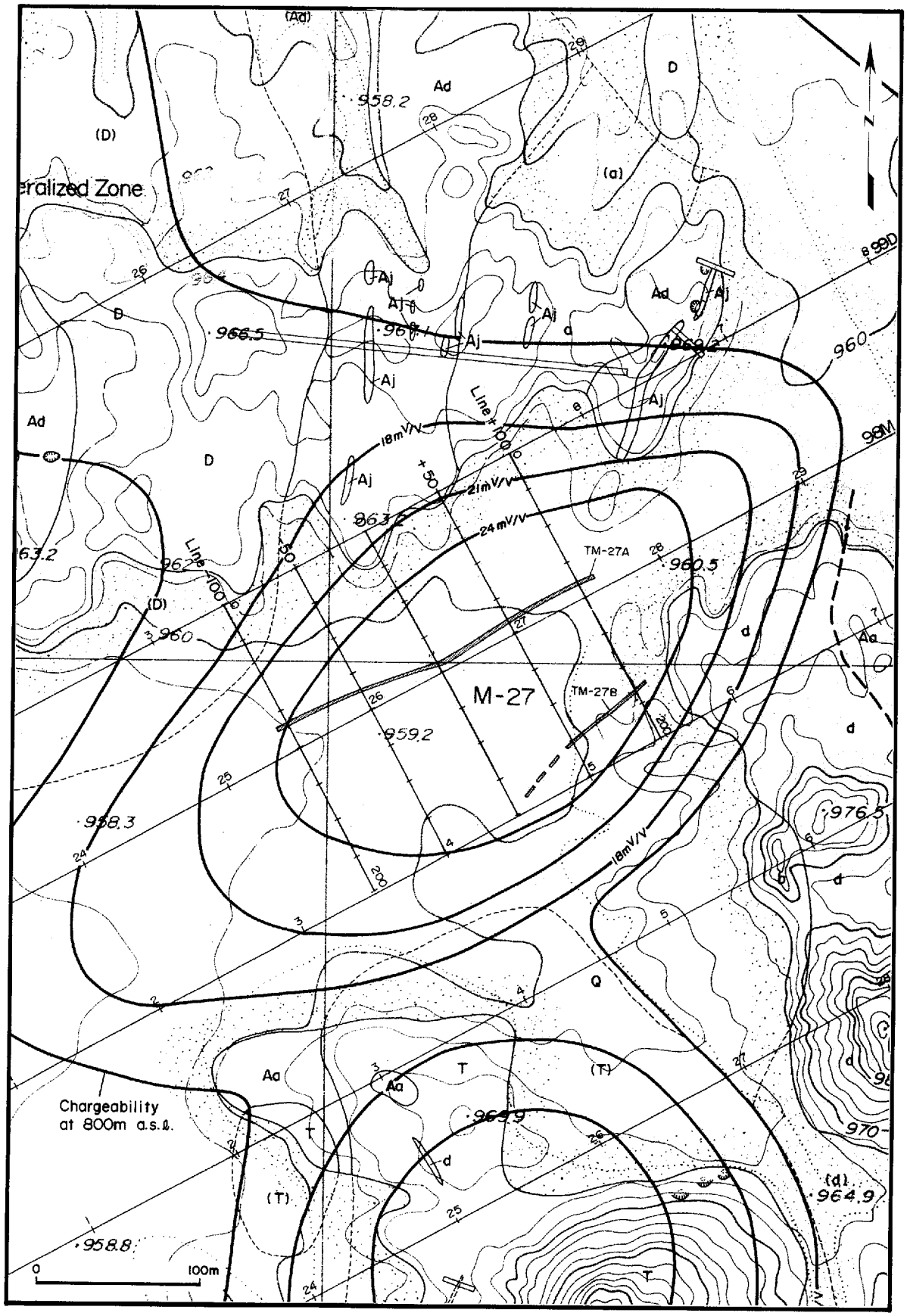

Fig.2-5-6 Integrated Interpretation Map of TM-27

5-4 TO-21 Sub-area

Geological map of the sub-area is shown in Figure 2-5-7, and the comprehensive interpretation map in Figure 2-5-8.

IP survey showed the highest chargeability values of 24mV/V at altitude of 800m (about 150m below the surface) near station 5 of IP traverse 99I. TEM survey resulted in the extraction of a N-S extending vertical conductive plate and it was named "TO-21A".

The subsurface geology of this sub-area is not clear because the TEM traverse lines are mainly over Quaternary sand and gravel bed. However, andesite of the Arj Group is exposed at the eastern and western end of the traverse lines and thus it is inferred that andesite and andesitic pyroclastic rocks occur in the subsurface zones of these traverse lines.

Drilling has not been carried out in TO-21 sub-area, but to the northeast of this sub-area, chalcopyrite-bearing quartz-calcite vein has been traced for 325m and assay result of the sample collected last year is as follows.

	Sample No.	Rock Name	Assay Result			
			Au (g/t)	Ag (g/t)	Cu (%)	Zn (%)
①	K9022006	30cm-wide quartz vein	<0.1	0.8	1.48	<0.01

The occurrence of rhyodacitic pyroclastic rocks cannot be expected in this sub-area, and thus the "TO-21A" is inferred to reflect vein-type mineralization.

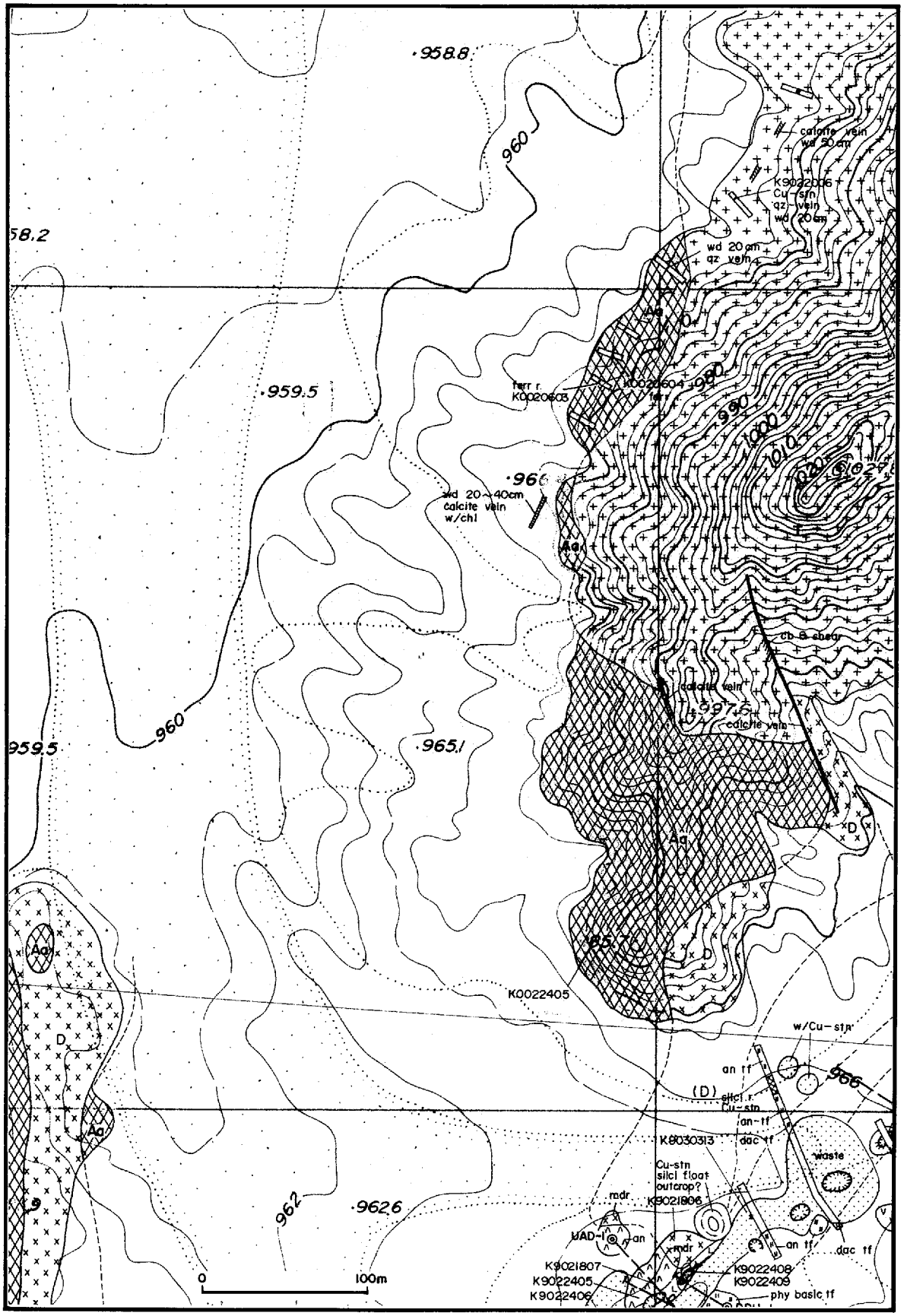

Fig.2-5-7 Detailed Geological Map of TO-21

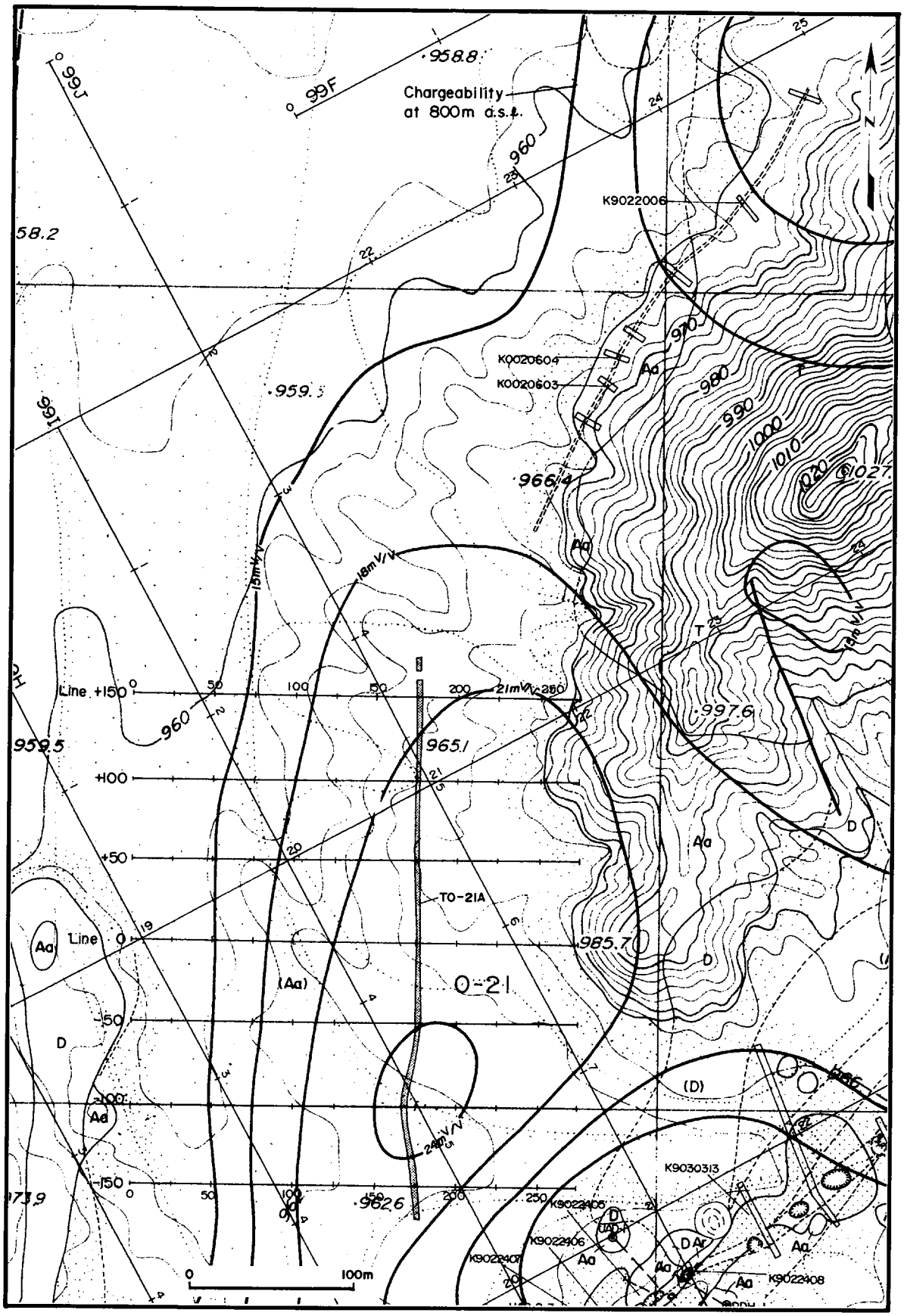

Fig.2-5-8 Integrated Interpretation Map of TO-21

5-5 TP-18 Sub-area

Geological map of the sub-area is shown in Figure 2-5-9, and the comprehensive interpretation map in Figure 2-5-10.

IP survey showed the highest chargeability values exceeding 21mV/V at altitude of 800m (about 150m below the surface) near station 18 of IP traverse 98P. TEM survey resulted in the extraction of NE-SW extending two vertical conductive plates and the northern plate was named "TP-18A" and the branching plate "TP-18B".

This sub-area is located to the southwest of the ancient pits of the South Prospect and it is covered mainly by Quaternary sand and gravel. Therefore the subsurface geology is not clear, but from geological information of trenches and nearby hills, it is inferred to consist of rhyodacite, dacite, andesite, and pyroclastic material of these rocks. UAD-4 and UAD-5 drilled by SEREM/US Steel in 1977 locate in the eastern margin of this sub-area. UAD-4 encountered mineralized zones at 105.95—115.00m and samples from this zone was re-assayed this time with the following results.

	Drilling Depth (m)	Interval (m)	Assay Result			
			Au (g/t)	Ag (g/t)	Cu (%)	Zn (%)
①	105.95—112.05	6.10	0.34	22.9	1.97	0.23
②	112.05—115.00	2.95	1.14	39.2	3.72	3.07

The mineralized zone of 105.95—112.05m depth interval consists of chalcopyrite-pyrite-quartz network and that of 112.05—115.00m consists of sphalerite-chalcopyrite-pyrite dissemination in chloritized rock, and the Au grade is high. The samples collected during the first year from the ancient pits of the South Prospect (K99022404 and K9030313) contain 6.2g/t and 3.0g/t Au, respectively. From the above, it is concluded that the mineralization of this sub-area is vein-type Au-Cu-Zn.

Exposed rocks occur to the west of conductive plate TP-18A extracted by TEM, and mineralization is not observed in the exposures although 1.0m wide quartz rocks occurs within chloritized andesite. On the other hand, plate TP-18B is located at the southwestern extension of the mineralized zone which extends in the NE-SW direction from the ancient pits of the South Prospect through UAD-4. Thus TP-18B is considered to reflect the existence of vein-type Au-Cu-Zn mineralization.

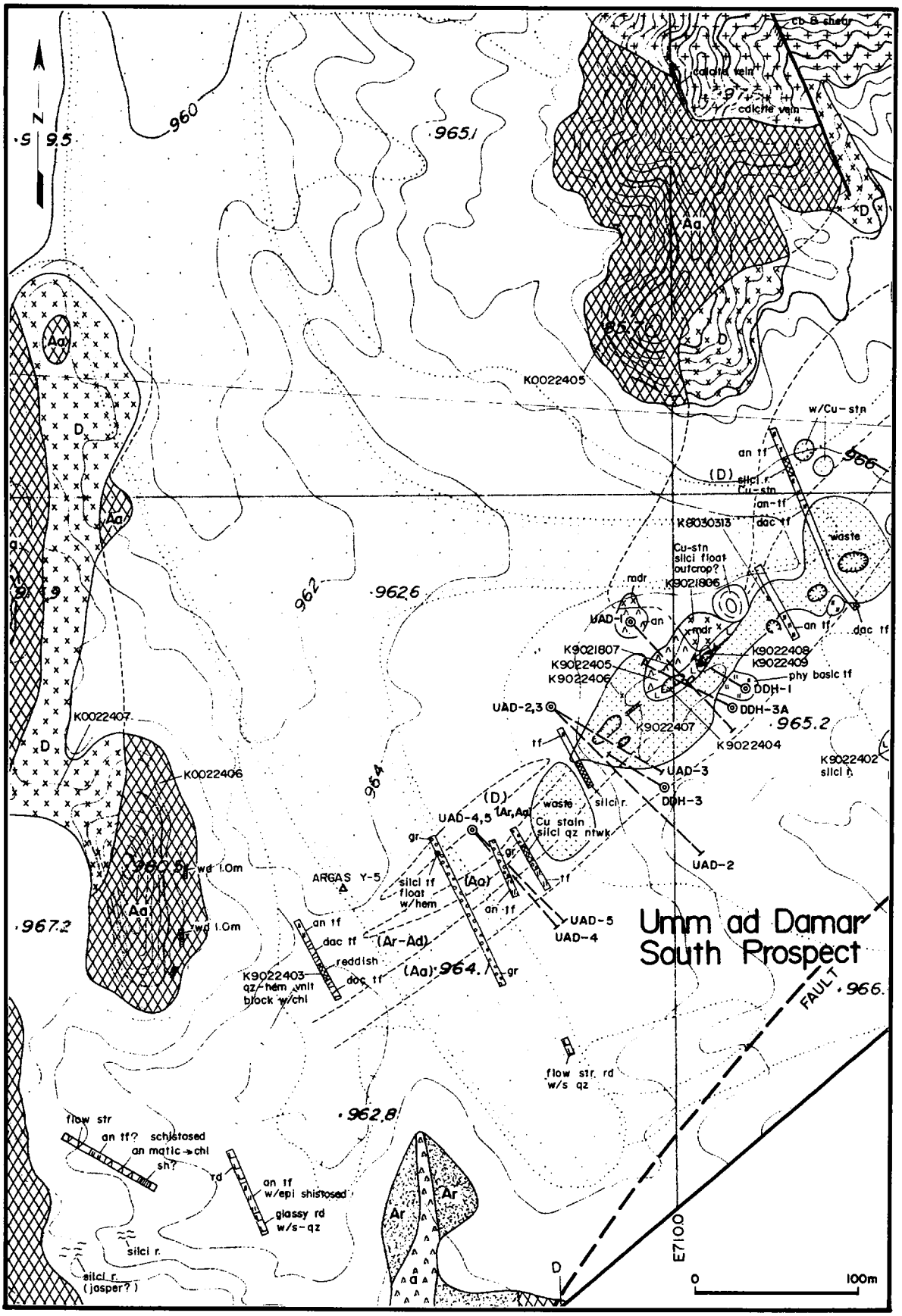

Fig.2-5-9 Detailed Geological Map of TP-18

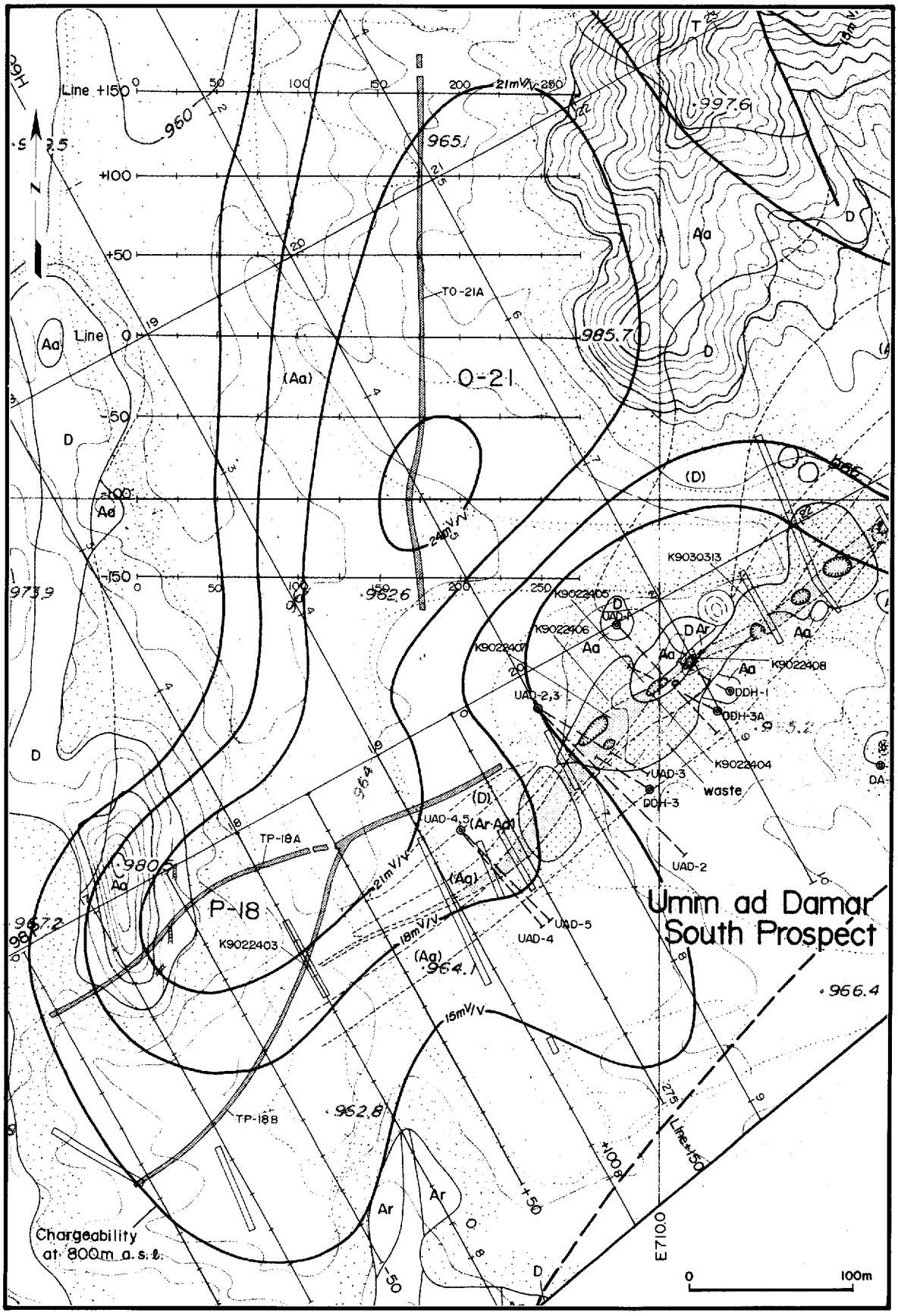

Fig.2-5-10 Integrated Interpretation Map of TP-18

PART III CONCLUSIONS AND RECOMMEMDATIONS

PART III CONCLUSIONS AND RECOMMEMDATIONS

CHAPTER 1 CONCLUSIONS

Drilling, detailed geological survey, IP and TEM geophysical survey were carried out in the Umm ad Damar area during the second year of the project. The results are summarized as follows.

① At total of eight holes with total length of 2,152m were drilled. The drilling sites were selected from the results of the first-phase detailed geological survey on known prospects and of IP reconnaissance with 300m traverse interval.

② Drilling clarified the existence of volcanogenic massive sulfide Cu-Zn mineralization at Jabal Sujarah, 4/6 Gossan, and a part of the North Prospect, also Cu vein mineralization was found to occur at the North Prospect.

③ Volcanogenic massive sulfide mineralization was confirmed at MJSU-2, MJSU-5, MJSU-6, and MJSU-8. In these holes, massive ore and breccia ore consisting of chalcopyrite-sphalerite-pyrite occur in host rock of rhyodacitic pyroclastic rocks. Shale and tuff are intercalated in the mineralized zones. Alteration of the host rock is silicification and chloritization. The main mineralized zones are as follows.

Drill Hole No.	Drilling Depth (m)	Interval (m)	Assay Result			
			Au (g/t)	Ag (g/t)	Cu (%)	Zn(%)
MJSU-2	121.15—125.40	4.25	0.37	23.0	0.96	2.17
	130.10—142.25	12.15	0.37	14.0	1.00	3.67
MJSU-5	268.90—275.40	6.50	<0.05	2.1	0.99	0.20
MJSU-6	134.75—138.00	3.25	<0.05	28.0	0.69	3.84
MJSU-8	73.25—73.55	0.30	<0.05	3.9	0.90	12.74
	82.65—83.35	0.70	0.24	19.5	1.57	0.01

④ Cu vein mineralization was confirmed at MJSU-3, MJSU-4, and MJSU-5 of the North Prospect. The veins and network mineralization observed in these holes consist of chalcopyrite and pyrite. The host rocks are dacite and dacitic pyroclastic rocks. The veins and network contain little silicate and oxide minerals. Chloritization is notable near the veins. Gold and silver grade is low. The main mineralized zones are as follows.

Drill Hole No.	Drilling Depth (m)	Interval (m)	Assay Result			
			Au (g/t)	Ag (g/t)	Cu (%)	Zn (%)
MJSU-3	220.10—220.90	0.80	<0.05	6.6	2.48	0.03
MJSU-4	140.50—147.80	7.30	<0.05	9.1	1.98	0.03
	155.50—158.85	3.35	<0.05	6.3	2.19	0.07
MJSU-5	79.40—82.55	3.15	0.07	15.4	2.25	0.06
	88.90—93.20	4.30	<0.05	13.7	1.93	0.03
	95.50—99.90	4.40	0.06	12.5	3.70	0.02
	245.65—247.70	2.05	<0.05	2.0	1.02	0.02
	328.90—331.20	2.30	0.07	7.1	6.51	0.01

⑤ The cores (drilled in 1977) stored in Jabal Sayid camp were re-arranged. And UAD-3, UAD-4, UAD-6, and UAD-10 cores were examined. Chalcopyrite-pyrite-quartz veins were observed at 105.95—112.05m depth and pyrite-chalcopyrite-sphalerite dissemination at 112.05—115.00m depth of UAD-4 of the South Prospect. The host rocks were chloritized rocks. The results of assay are as follows.

Drill Hole No.	Drilling Depth (m)	Interval (m)	Assay Result			
			Au (g/t)	Ag (g/t)	Cu (%)	Zn (%)
UAD-4	105.95—112.05	6.10	0.34	22.9	1.97	0.23
	112.05—115.00	2.95	1.14	39.2	3.72	3.07

Ore samples collected from ancient pits of this Prospect also showed 3.0—6.2 g/t Au. It is seen that the mineralization of this Prospect has higher Au and Zn content than the Cu veins of the North Prospect.

⑥ IP geophysical survey was carried out in order to clarify the detailed chargeability distribution of the "B-12", "M-27", and "P-18" anomalous zones extracted by IP survey first year. The following was clarified as a result.

B-12 anomaly: The lateral extension of this anomalous zone is the largest in the survey area, and the chargeability is very high.

M-27 anomaly: This anomalous zone consists of northern and southern sub-zones. The northern strong anomaly sub-zone including station M-27 is oblong and

extends in the NE-SW direction. The southern sub-zone occurs around station N-25 and is small.

P-18 anomaly: This anomalous zone extends northward and connects with station O-21.

⑦ Five sub-areas were selected for TEM geophysical survey. They are TB-12, TJ-18, TM-27, TO-21, and TP-18. Selection was based on IP survey and detailed geology. TEM survey resulted in extracting almost vertical conductive plates in these sub-areas.

⑧ The results of detailed geological survey, drilling, examination of existing cores, IP survey, and TEM survey were interpreted comprehensively. The conductive plates extracted in TM-27, TO-21, and TP-18 sub-areas are assessed to indicate vein-type mineralization and the plates in TB-12 and TJ-18 sub-areas volcanogenic massive sulfide mineralization.

CHAPTER 2 RECOMMENDATIONS FOR THE THIRD PHASE SURVEY

The following work is recommended for the third year of this project.

① Further drilling is recommended for the 4/6 Gossan in order to confirm the downward extension of the mineralized zone confirmed at MJSU-2.

② Occurrence of a new mineralized zone is anticipated from TEM results at Jabal Sujarah aside from that confirmed by MJSU-8. Further drilling is recommended in order to assess the mineralization of this sub-area.

③ Drilling is recommended for assessing the conductive plates extracted by TEM survey at TJ-18, TM-28, TO-21, and TP-18.

REFERENCES

REFERENCES

Bowen, R. A. and Smith, G. H., 1981. An Overview Study of the Jabal Sayid District: Technical Record RF-TR-01-2, 72p.

BRGM-OF-07-6 (Open-file Report). Review of Gold Mineralization in the Arabian Schield, 4/6 Gossan, Umm ad Damar District: 10p.

Chinkul, M., 1983. A Study of the Fluid Inclusions and O & H Stable Isotopes at Jabal Sayid and its Bearing on the Mineralization: Unpublished Ms.c. Thesis: Faculty of Earth Sci., King Abdul Aziz University, Jeddah, Kingdom of Saudi Arabia, 174p.

Conraux, J., 1969. Aqiq-Umm ad Damar Drilling Hole Results: BRGM 15p.

DGMR, 1994. Mineral Resources of Saudi Arabia: 322p.

Hakim, H. D. and Chinkul, M., 1989. A Fluid Inclusion Study on Mahd adh Dhahab Gold Deposit, Saudi Arabia: JKAU: Earth Sci., vol.2, pp.51-68.

Harvey T. V., 1984. Ground Geophysical Surveys at the Umm ad Damar Prospect, 1402 to 1404 Program (February 1982 to December 1983): Open-File Report RF-OF-04-12, 44p.

Howes, D. R., 1984. Mineral Exploration of the Umm ad Damar Prospect: 1403-1404 Program (March 1983 to January 1984), Open-File Report RF-OF-04-4, 44p.

Kemp, J., Gros, Y., and Prian, J., 1982. Explanatory Note to the Geologic Map of the Mahd adh Dhahab Quadrangle, Sheet 23E, Kingdom of Saudi Arabia: pp.1-39.

Lewis, P. J. and Martin, G. J., 1983. Mahd adh Dhahab Gold-silver Deposit, Saudi Arabia ,Mineralogical Studies Associated with Metallurgical Process Evaluation: pp.63-72.

Luce, R. W., O'Neil, J. R., and Rye, R. O., 1979. Mahd adh Dhahab: Precambrian Epithermal Gold Deposit, Kingdom of Saudi Arabia: U.S. Geological Survey (Saudi Arabian Project Report 256), 33p.

Ramsom, D. M., 1982. Geology and Mineralization of the Umm ad Damar South Prospect, Jabal Sayid District, Kingdom of Saudi Arabia :Riofinex Geological Mission, 59p.

Ramsom D. M., 1984. Regional Geology of the Umm ad Damar Area and Geology of the North Prospect: Open-File Report RF-OF-04-9, 23p.

RF-1979-9. 6.2 Umm ad Damar: pp.95-98.

Rye, R. O., Hall, W. E., Cunningham, C. G., Czamanske, G. K. Afifi, A. M., and Stacey, J. S., 1982. Preliminary Mineralogic, Fluid Inclusion, and Stable Isotope Study of the Mahd adh Dhahab Gold Mine, Kingdom of Saudi Arabia: Open-File Report USGS-OF-03-4, 26p.

Sabir, H., 1981. Metalogic and Textural Features of Sulfide Mineralization at Jabal Sayid (Saudi Arabia): Bulletin du BRGM Section II, no.1-2/1980-1981, pp.103-111.

Sahl, M. A., 1979. Geology and Mineralization at Umm ad Damar Area: Faculty of Earth Sciences, King Abdul Aziz University, pp.183-221.

PHOTOGRAPHS

Drill Hole No.: MJSU-7

Drill Hole No.: MJSU-7

Photo. 1　Photographs of Drilling Exploration

IP Survey: SCINTREX IPR-12
Time Domain IP/Resistivity Receiver

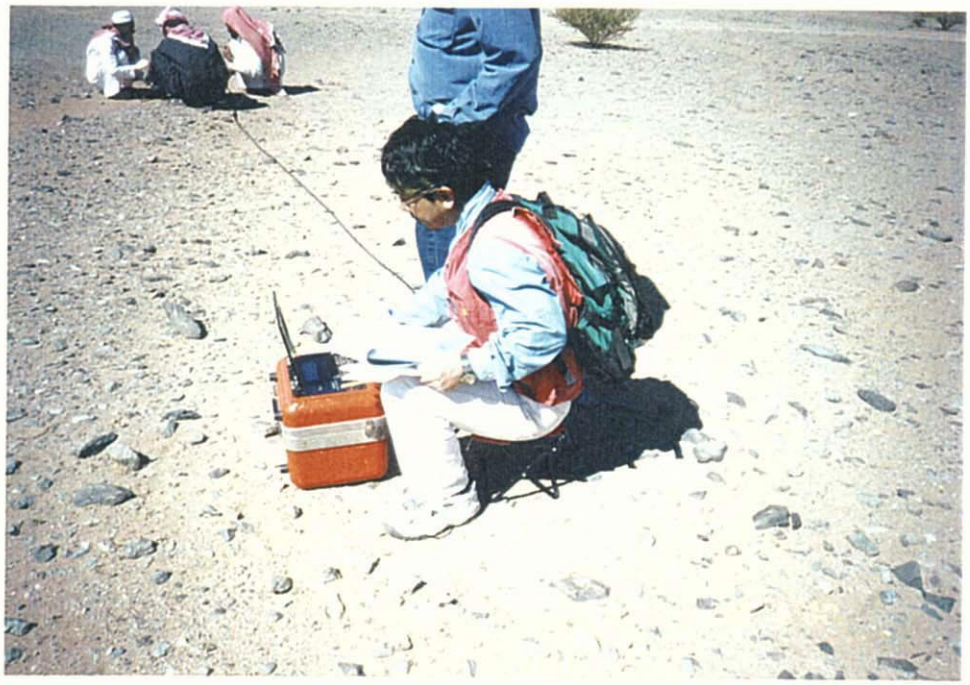

TEM Survey: GEONICS PROTEM Receiver

Photo. 2 Photographs of Geophysical Survey

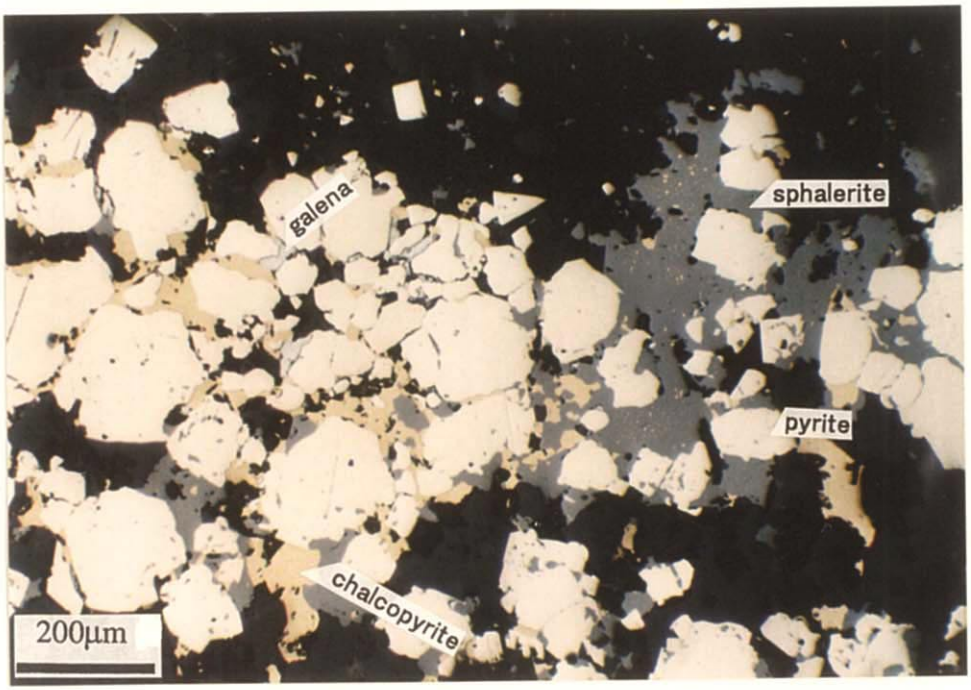

(Open Nicol)

Drill Hole No.: MJSU-2
Sample No.: 124P
Sampling Depth: 124.3m
Type of Ore: Breccia Ore

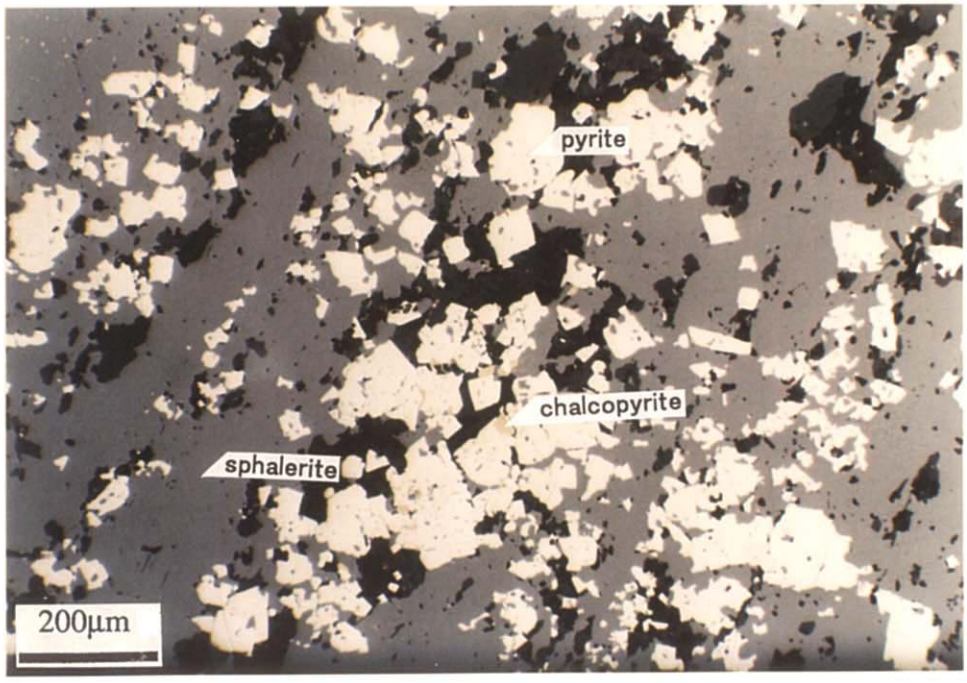

(Open Nicol)

Drill Hole No.: MJSU-2
Sample No.: 132P
Sampling Depth: 132.1m
Type of Ore: Massive Ore

Photo. 3 Photomicrographs of Ores